Hydrothermally Synthesized Sulfur and Phosphorus-Doped Ternary Metal Electrocatalysts for Efficient Hydrogen Evolution Reaction

Tadiwos Melaku Kebede

A Thesis submitted to

The Department of Chemical Engineering

College of Mechanical, Chemical and Materials Engineering

Presented in Partial Fulfillment of the Requirement for Degree of

Master's in Chemical Engineering (Process Engineering)

Office of Graduate Studies

Adama Science and Technology University

May, 2025

Adama, Ethiopia

Hydrothermally Synthesized Sulfur and Phosphorus-Doped Ternary Metal Electrocatalysts for Efficient Hydrogen Evolution Reaction

Tadiwos Melaku Kebede

Advisor: Dr. Tadele Negash Gemeda

Co- Advisor: Dr. Zelalem Tumsa Tefera

A Thesis Submitted to

The Department of Chemical Engineering

College of Mechanical, Chemical and Materials Engineering

Presented in Partial Fulfillment of the Requirement for Degree of Master's in Chemical Engineering (Process Engineering)

Office of Graduate Studies

Adama Science and Technology University

May, 2025

Adama, Ethiopia

DECLARATION

I hereby declare that this Master thesis entitled **"Hydrothermally Synthesized Sulfur and Phosphorus-Doped Ternary Metal Electrocatalysts for Efficient Hydrogen Evolution Reaction"** is my original work and has not been submitted to any university for a similar purpose. The reference used in this thesis are duly recognized by appropriate citation

Tadiwos Melaku		
Name of student	Signature	Date

RECOMMENDATION OF ADVISOR

We hereby certify that we have closely advised the student while developing this thesis and read the revised version of the thesis entitled **"Hydrothermally Synthesized Sulfur and Phosphorus-Doped Ternary Metal Electrocatalysts for Efficient Hydrogen Evolution Reaction"** prepared under our guidance by Tadiwos Melaku. Therefore, we recommend the submission of the thesis to the department following the applicable procedures.

Dr. Tadele Negash	_____	_____
Major Advisor	Signature	Date
Dr. Zelalem Tumsa	_____	_____
Co-advisor	Signature	Date

APPROVAL SHEET

We hereby certify that the recommendation and suggestion given by the thesis review committee are appropriately incorporated into the final thesis entitled **"Hydrothermally Synthesized Sulfur and Phosphorus-Doped Ternary Metal Electrocatalysts for Efficient Hydrogen Evolution Reaction"** by Tadiwos Melaku.

Dr. Tadele Negash	_____	_____
Major Advisor	Signature	Date
Dr. Zelalem Tumsa	_____	_____
Co-advisor	Signature	Date

APPROVAL OF BOARD OF REVIEWER

We, the undersigned, members of Board of the Reviewers of open defense by Tadiwos Melaku have read and evaluated the thesis entitled **"Hydrothermally Synthesized Sulfur and Phosphorus-Doped Ternary Metal Electrocatalysts for Efficient Hydrogen Evolution Reaction***"* and assessed the understanding of the candidate about the proposed research. This is, therefore to certify that the thesis is accepted for partial fulfillment of the requirement of the degree of science in Process Engineering.

Chairperson	Signature	Date
Internal Examiner	Signature	Date
Dr. Sintayehu Mekuria External Examiner	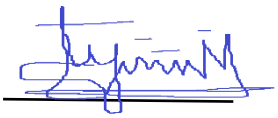 Signature	Date

Final approval and acceptance of the thesis is contingent upon the submission of its final copy to the Office of Post Graduate Studies (OPGS) through the Department Graduate Council (GDC) and School Graduate Committee (SGC).

Department Head	Signature	Date
Dean	Signature	Date
Office of Post Graduate Studies, Dean	Signature	Date

ACKNOWLEDGEMENT

First and foremost, I express my deepest gratitude to God and Theotokos for the divine guidance, strength, and grace throughout this journey.

I am sincerely thankful to my advisor, Dr. Tadele Negash, for his continuous guidance, insightful supervision, and invaluable feedback. His experience in electrochemical systems greatly shaped the scientific direction, methodology, and overall writting of this work. I also extend my heartfelt appreciation to my co-advisor; Dr. Zelalem Tumsa, his critical understanding of how to approach, conduct and write scientific research has greatly strengthened both the content and presentation of this thesis and deepened my understanding of the research process.

Special thanks to Mr. Biruk Sisay and his team at Changwon National University, Korea, as well as to Mr. Tariku Ayala, Mr. Kefyalew Hailemariam and their team at National Taiwan University of Science and Technology for their valuable contribution in the characterization process.

Finally, I am deeply grateful to my family and friends for their unwavering love, patience, and encouragement, which have been a constant source of strength.

Table of Contents

DECLARATION ii
RECOMMENDATION OF ADVISOR iii
APPROVAL SHEET iv
APPROVAL OF BOARD OF REVIEWER v
ACKNOWLEDGEMENT v
List of Tables ix
List of Figures x
List of Acronyms xi
Abstract xii
CHAPTER ONE 1
INTRODUCTION 1
1.1 Background 1
1.2 Statement of Problem 4
1.3 Research Question, Choice of the system and Hypothesis 5
1.3.1 Research Question 5
1.3.2 Choice of System 5
1.3.3 Research Hypothesis 5
1.4 Research Objectives 6
1.4.1 General Objective 6
1.4.2 Specific Objective 6
1.5 Significance of the study 6
1.6 Scope of the study 7
1.7 Limitation of the study 7
1.8 Organization of the thesis 8
CHAPTER TWO 9
LITERATURE REVIEW 9
2.1 Introduction 9
2.2 Global Energy Landscape and the History of Energy Transition 10
2.3 Ethiopia's Renewable Energy Landscape: Progress and Potential 12
2.4 The Role of Green Hydrogen in Advancing the Renewable Energy Economy 15
2.5 Green Hydrogen Production via Water Electrolysis 16
2.5.1 Alkaline Water Electrolysis (AWE) 17
2.5.2 Acidic (PEM) Water Electrolysis 17
2.6 Fundamental Mechanisms in Alkaline Water Electrolysis and the Hydrogen Evolution Reaction (HER) 18
2.6.1 Basic Mechanism of Alkaline Water Electrolysis 18
2.6.2 Detailed Electrochemical Steps of the Hydrogen Evolution Reaction (HER) in Alkaline Media 19
2.7 Electrocatalysts for Efficient HER in Alkaline Electrolysis 20
2.8 Hydrothermal Synthesis of Electrocatalysts for Enhanced HER Activity 21
2.8.1 Principles and Advantages of Hydrothermal Synthesis Techniques 21
2.8.2 Recent Applications of Hydrothermal Methods in Synthesizing HER Catalysts 22
2.9 Alternative Synthesis Methods 22
2.9.1 Microwave synthesis 22
2.9.2 Sol-Gel Method 23
2.9.3 Electrodeposition 25
2.9.4 Chemical Reduction 25

2.9.5 Emerging Electrocatalyst Synthesis Methods 28
2.10 State-of-the-Art Noble Metal-Based Catalysts: Performance and Limitations ...29
2.11 Transition Metal-Based (Non-Noble) Catalysts: An Overview of Recent Progress 30
2.11.1 Recent Studies on Ni-Mo-V Catalysts for Alkaline HER....31
2.12 In-situ and Ex-situ Characterization Techniques for Analyzing HER Electrocatalysts 34
2.12.1 Common Ex-situ Techniques for Structural and Morphological Analysis 34
2.12.2 Electrochemical Methods for Evaluating Catalytic Activity and Performance 34
2.12.3 Advanced In-situ Techniques for Understanding Reaction Mechanisms and Catalyst Evolution....35
2.13 Challenges and Future Perspectives in the Development of Efficient HER Electrocatalysts 35
2.13.1 Current Limitations and Bottlenecks in Non-Noble Metal Catalysis 35
2.13.2 Promising Future Research Directions for Achieving High-Performance and Durable HER Catalysts 36
CHAPTER THREE 38
MATERIALS AND METHODS 38
3.1 Chemicals and Materials....38
3.1.1 Chemicals 38
3.1.2 Equipments....38
3.2 Experimental Design 39
3.2.1 Design Strategy of (Ni, Mo, V)-P, S Electrocatalysts 39
3.2.2 Hydrothermal Synthesis of (Ni, Mo, V)-P, S and Controlled Samples 40
3.2.3 Hydrothermal Synthesis of Controlled Samples 42
3.3 Characterization 42
3.3.1 Structural, Morphological and Compositional Characterization....42
3.3.2 Electrochemical Characterization....43
3.3.3 Electrochemical set up 46
CHAPTER FOUR....49
RESULT AND DISCUSSION....49
4.1 Introduction....49
4.2 Structural Characterization 49
4.3 Morphology analysis 51
4.4 Surface Elemental Composition and Chemical State Analysis 55
4.5 Electrochemical analysis....57
4.5.1 Effect of Phosphorus Doping on HER Electrocatalytic Performance 57
4.5.2 Effect of Sulfur Doping on HER Electrocatalytic Performance 59
4.5.3 Electrolytic performance of (Ni, Mo, V)-P, S and controlled samples....61
4.5.3.1 LSV 61
4.5.3.2 EIS....63
4.5.3.3 Tafel analysis 64
4.5.3.4 Constant Voltage....65
CHAPTER FIVE 68
CONCLUSION AND RECOMMENDATION 68
5.1 Conclusion 68
5.2 Recommendation for future work 69
REFERENCES 70

List of Tables

Table 2. 1: Domestic renewable energy source potentials and consumption status (Guta & Börner, 2017; Khan & Singh, 2017; G. A. Tiruye et al., 2021) 12
Table 2. 2: Summary of alternative electrocatalyst synthesis methods 26

Table 3. 1: Equipment and apparatus used during the study.....38
Table 3. 2: Concentration matrix used during anionic regulation 39

Table 4. 1: EDS quantitative results 54
Table 4. 2: Effect of Phosphorus Doping Concentration on the HER Performance of NiMoVP-x Electrocatalysts.....57
Table 4. 3: Effect of Sulfur Doping Concentration on the HER Performance of NiMoVPS-x Electrocatalysts 59
Table 4. 4: Comparison of the electrocatalytic activity of the synthesized (Ni, Mo, V)-P, S heterostructure toward HER with previously reported high entropy electrocatalysts. 67

List of Figures

Figure 2. 1: Visual Chapter Outline 10
Figure 2. 2: Key worldwide expansion trends and contributions to energy consumption by type in 2024 (Alex Martinos, 2025) 12
Figure 2. 3: Ethiopian energy demand forecast (G. Tiruye et al., 2021) 13
Figure 2. 4: Demand for hydrogen per sector in 2023, the Stated Policies Scenario, and the 2030 Net Zero Emissions by 2050 Scenario (Giovanni Andrean et al., 2025) 16
Figure 2. 5: Microwave heating (Alex Martinos, 2025) 23
Figure 2. 6: Schematic representation of sol–gel synthesis of M1X-M2X/N82 and M1X-M2X/XC72 electrocatalysts (Petkucheva et al., 2025) 24
Figure 2. 7: Schematic of the Co-P nanocluster generation by electrodeposition (J. Kim et al., 2023) 25
Figure 2. 8: Formation of Ni2S2 PN/NF composite (P. Zhu et al., 2024) 31
Figure 2. 9: Schematic illustration of the 3-D NiMo electrocatalyst surface (Fang et al., 2016) 32

Figure 3. 1: Pretreatment of nickel foam 41
Figure 3. 2: Preparation of hydrothermal precursor solution 41
Figure 3. 3: (a) Electrochemical characterization set up (b) Three electrode system 47
Figure 3. 4: Schematic representation of electrochemical characterization set up 47

Figure 4. 1: (a) XRD patterns (b) magnified XRD of (Ni, Mo, V)-P, S 51
Figure 4. 2: SEM image (a) 100 x (b) 500 x (c) 3.00 kx (d) 10.00 kx (e) 20.00 kx(f) 80.00 kx 53
Figure 4. 3: (a) SEM , EDS for (b) Oxygen (c) Phosphorus (d) Molybdenum (e) Sulfur (f) Vanadium (g) Nickel 54
Figure 4. 4: XPS (a) Mo 3d (b) Ni 2p (c) O 1s (d) (e) S 2p (f) V 2p 57
Figure 4. 5: LSV on effect of phosphorus doping on HER performance 59
Figure 4. 6: LSV on effect of sulfur doping on HER performance 61
Figure 4. 7: (a) LSV (b) Overpotential 63
Figure 4. 8: Electrochemical Impedance Spectroscopy (EIS) 64
Figure 4. 9: Tafel plot 65
Figure 4. 10: Constant voltage characterizations of (Ni, Mo, V)-P, S 66

List of Acronyms

HER	Hydrogen Evolution Reaction
OER	Oxygen Evolution Reaction
Ni	Nickel
V	Vanadium
MW	Megawatt
GW	Gigawatt
SDGs	Sustainable Development Goals
AWE	Alkaline Water Electrolysis
NH_3	Ammonia
HCl	Hydrochloric Acid
AHW	Atomic Hydrogen Welding
TMP	Transition Metal Phosphides
CC	Carbon Cloth
NS	Nanosheets
LSV	Linear Sweep Voltammetry
EIS	Electrochemical Impedance Spectroscopy
CV	Cyclic Voltammetry
SEM	Scanning Electron Microscope

Abstract

The growing demand for energy along with the environmental impact and potential scarcity of fossil fuels has underscored the urgent need for alternative energy carriers. Green hydrogen is a clean and high-energy alternative, but its adoption is hindered by the limited availability and high cost of platinum-group metals (PGM). To address this challenge, the present study aims to develop multi-element transition metal electrocatalysts doped with non-metals for effective hydrogen evolution reaction (HER). In this work, a sulfur and phosphorus co-doped ternary metal electrocatalyst (Ni, Mo, V)-P, S was synthesized via a one-step hydrothermal method using nickel foam as a substrate. The synthesized catalyst was characterized using X-ray diffraction (XRD), which confirmed the formation of crystalline Ni-based phases and revealed structural changes induced by phosphorus and sulfur doping, which influence catalytic behavior. Scanning electron microscope (SEM) revealed extremely rough surface with uniform deposition on the 3D porous structure of the nickel foam, promoting increased surface area. Energy dispersive X-ray Spectroscopy (EDS) confirmed the presence of Ni, Mo, V, S, and P elements, while X-ray Photoelectron Spectroscopy (XPS) further confirmed the presence of nickel, molybdenum, vanadium and sulfur and provided evidence of favorable chemical states. The (Ni, Mo, V)-P,S catalyst showed superior HER activity requiring an overpotential of only -53 mV at 10 mAcm^{-2}, and electrochemical impedance spectroscopy (EIS) revealed a low charge transfer resistance of 1.2 Ω, which shows rapid electron transfer at the electrode–electrolyte interface. The electrocatalyst showed a sustained operation for ~ 30,000 seconds under high current density of 100 mAcm^{-2}, confirming consistent operational stability without significant degradation. These findings emphasize the effectiveness of co-doping and ternary metal synergy in regulating the electronic structure and HER kinetics, making the (Ni, Mo, V)-P, S catalyst a promising alternative to PGM for efficient hydrogen evolution in alkaline water electrolysis.

Keywords: Hydrogen Evolution Reaction (HER), Hydrothermal Synthesis, Multi-element co-doping, Water Electrolysis, Transition Metal Synergy, Electrocatalytic activity, Electrocatalyst, Stability

CHAPTER ONE
INTRODUCTION

1.1 Background

Energy is the soul that gives life for all operations in the modern world, from cooking food, watching television, and charging our phones to transportation, manufacturing and industrial processes. It is a fundamental entity that exists in various forms and originates from sources like molecules (fossil fuels and biomass), atoms (nuclear), and photons (solar). Ever since it was first utilized by human beings, energy has been a driving force for growth and has directly promoted great advancements in the development of human civilization (Tiba et al., 2017).

Throughout history, there have been energy transitions marking significant turning points in the functioning of society as humanity moves toward ever more efficacious forms of energy. The shift of primary energy source is an issue with civilization that has continued with time (Yang et al., 2024). At present, and in the ongoing process of transition in energy sources, more use being given to renewable and carbon free energy sources like solar, hydropower, wind, etc (Khan et al., 2019). This phase of energy transition historically began following the global oil crisis of the 1970s, a trend that drove countries to pursue investigations into possible new and alternative sources of energy that could offer greater sustainability and degree of reduction from total dependence on oil (Yang et al., 2024).

In 1982 the German Institute of Applied Ecology published the first book putting forward the idea of energiewende or energy transition. It argued for a future energy system that would make extensive use of renewable sources instead of oil and nuclear energy. This is some early version of what one might call a renewable energy transition (Yang et al., 2024). Initially, the oil crisis served as a big push; however, the motives for the energy transition have since evolved. Present motives include limiting the environmental effect of fossil fuel usage, securing energy, availability and affordability (Genc & Kosempel, 2023). Recent events such as the Russain-Ukrainian conflict have given an enhanced rationale to the energy transition as one that is crucial for energy security (Genc & Kosempel, 2023).

Significant alternative prospects are presented for the world due to the shift towards renewable energy. The energy transition contributes to energy security through a decrease in dependence upon climate susceptible and geographically concentrated fossil fuel resources. Renewable energy sources are generally more dispersed, thereby ensuring greater energy independence and a higher resistance to volatility in global energy markets. A more diversified energy mix inclusive of renewable energy strengthens a nation's energy infrastructure and diminishes its vulnerabilities (Genc & Kosempel, 2023).

In spite of several opportunities, the renewable energy transition is facing a few challenges, especially those relating to the inherent seasonality of many renewable energy resources. This variability in availability will pose challenges to ensuring the security and reliability of the supply of energy. Solar energy production relies on sunlight and varies with the time of the year and the changing intensity and duration of sunlight during the day. To illustrate, solar generation peaks in the early afternoon, whereas peak electricity demand occurs in the late evening. This temporal disparity could cause excessive generation during off-peak hours and a possible supply shortage during the peak demand hours, with seasonal variations affecting both renewable resource availability and energy consumption patterns (e.g., increased electrical demand for heating in winter or cooling in summer).Wind energy relies on wind patterns that differ considerably during the seasons. This basically means that these renewables may be in scarcity at times of high energy demand or at times become surplus in low demand (Mikulčić et al., 2021).

Green hydrogen has been seen as a better alternative for transitioning the energy-intensive sectors in to carbon free system. Being identified as an attractive means of long-term energy storage, green hydrogen constitutes an excellent option. While renewable energy generation surpasses demand (during peak sunlight and high winds), surplus energy is fed into the electrolyzers for electrolysis to separate water into hydrogen and oxygen (Angelico et al., 2025). Thereafter, hydrogen could be stored and reversed back to electricity with the aid of fuel cells or turbines when there is low production from renewable energy sources or high consumption of energy by the customers. This process enables grid balancing as well as continuing supply of energy (Chigbu & Nweke-Eze, 2023).

However, Green hydrogen has relatively higher production cost than the conventional hydrogen. The electrolyzer costs make up the largest share of green hydrogen production expenses, somewhere around 40-60% of total cost. These high initial capital investment dynamics directly bear the load on green hydrogen production. The developments of effective electrocatalysts are profoundly significant in influencing the performance and cost-effectiveness of these advanced technologies (Ďurovič et al., 2021).

Hence, this study aims to develop a material that yields excellent activity at low cost and abundantly. As the success of these catalysts can lead to an actual reduction in material costs related to the electrolyzer itself, it will also enable a cheaper production of green hydrogen on a larger scale. This thesis expands on the results obtained by previous researchers who have studied the potential of transition metals for replacement of noble metals. It provides an original contribution to the field insomuch as it tackles previously understudied area of multi element transition metal catalysts for effective electrochemical hydrogen evolution reaction (HER).

The selection of the metal elements of the electrocatalyst is based on their combined electrocatalytic properties. Nickel is abundant, cheap, and exhibits good HER activity in alkaline media due to its favorable hydrogen binding energy and high electrical conductivity (Angeles-Olvera et al., 2022). It does have the disadvantage of moderate HER activity and surface oxidation. Molybdenum enhances electron transfer, forms Mo-based active phases, and improves the overall stability of the catalyst; still, it has poor conductivity and low electrocatalytic performance for HER (Baltrusaitis et al., 2015). Vanadium serves to create redox-active sites, enhances charge transfer, and increases defect density; yet it is less efficacious for HER and is not very stable in alkaline media (Bouzbib et al., 2023). Each of them suffers limitations on their own; their combination, however, forms a synergic system in which the proficiency of one component negates the other's limitations. For example, Bau et al. (2020) reports that during the HER catalysis on Ni-Mo catalysts, molybdenum species play an important role as the active sites, while nickel assists by dispersing and activating molybdenum species (Bau et al., 2020).

In addition to metal synergy, dual doping with sulfur (S) and phosphorus (P) additionally optimizes the performance of the catalyst. Sulfur doping induces lattice distortion, generates surface defects, and forms desirable metal–sulfur bonds that increase the number density of electroactive sites (Liu et al., 2021). However, sulfur

may reduce conductivity and stability of sulfide phases in alkaline solutions. Phosphorus doping, on the other hand, increases electron density at metal sites, total conductivity, and modifies hydrogen adsorption energy but may undergo oxidation or leaching which leads to loss of active sites if not constrained by suitable metal substrates (Jia et al., 2023). S and P co-doping avoids these individual limitations, S increases surface roughness and accessibility of active sites and P increases electron mobility and charge transfer efficiency (Xu et al., 2024). They together display a synergistic effect that provides both electrochemical stability and catalytic kinetics for long-term operation. The ternary metal system and dual non-metal doping strategy combination therefore produces a stable and efficient electrocatalyst for hydrogen evolution in alkaline water electrolysis.

1.2 Statement of Problem

Ethiopia faces significant energy challenges, including low per capita energy supply and heavy dependence on imported petroleum, which consumes 10–14% of its import budget and contributes to 15–18% of external public debt (Yalew, 2022). This dependency exposes the country to energy insecurity, price volatility, and supply risks.

Ethiopia, the land tagged as the “Water Tower of Africa”, has the potential to adopt hydrogen-based energy, yet lacks affordable catalyst alternatives. The country’s rich hydrological endowment coupled with diverse and abundant renewable energy resources positions it advantageously for green hydrogen production via water electrolysis. However, the absence of locally available, low-cost, and effective catalytic materials hinders the realization of this potential. Without alternatives to platinum-group metals, the transition to a hydrogen economy remains economically out of reach for Ethiopia and similar developing nations.

This limitation necessitates the development of alternative, earth-abundant electrocatalysts which can be less costly and favorable for alkaline water electrolysis. Recent studies have focused on binary and ternary transition metal-based electrocatalysts or on single-dopant strategies, which have shown promising HER activity. However, their performance still falls short of that achieved by PGM-based catalysts, particularly in terms of catalytic activity.

To bridge this gap, multi-element doping has, therefore, been recently proposed and explored as a promising strategy to enhance the performance of transition metal-based electrocatalysts. Non-metal dopants such as sulfur and phosphorus can tune the structure, modify morphology, and introduce surface defects thus enhancing catalytic activity and charge transfer processes. Despite these advantages, co-doping on multi-element systems such as (Ni, Mo, V)-based materials with S and P yet remains relatively unexplored, especially for alkaline conditions. Therefore, this study aims to synthesize and evaluate sulfur- and phosphorus-doped (Ni, Mo, V)-based electrocatalysts, prepared via a hydrothermal method, for improved HER performance in alkaline media.

1.3 Research Question, Choice of the system and Hypothesis

1.3.1 Research Question

The research aims to address three key questions:

1. Can a transition metal-based (Ni-Mo-V) electrocatalyst be synthesized using hydrothermal methods to exhibit efficient HER activity in alkaline media?
2. What structural and surface features, morphology and chemical state, of the (Ni, Mo, V)-P, S electrocatalyst contribute to its hydrogen evolution reaction (HER) performance in alkaline media?
3. Does the incorporation of sulfur (S) and phosphorus (P) improve electrochemical properties of Ni-Mo-V electrocatalysts for HER?

1.3.2 Choice of System

The study focuses on alkaline water electrolysis because the alkaline solution allows using low cost transition metals. Despite acidic media offering better performance, alkaline media is preferred due to its lower corrosion rates, reduced safety risks, and compatibility with a broader range of transition metals (Sebbahi et al., 2024) (Wang et al., 2021).

1.3.3 Research Hypothesis

The modification of Ni-based electrocatalyst by growing Ni, Mo, V, P and S on Ni foam is expected to enhance their performance in Hydrogen Evolution Reaction (HER). The synergistic effect of these elements improves the electrocatalysts performance. Nickel acts both as an additional electrocatalyst and a substrate,

providing a robust foundation. Molybdenum optimizes hydrogen kinetics, vanadium enhances conductivity and electron density, and phosphorus and sulfur refine surface chemistry for greater efficiency. This combination results in a more effective catalyst for sustainable energy application.

1.4 Research Objectives

1.4.1 General Objective

The main aim of this research is to develop multi-element transition metal catalysts doped with non-metals using the hydrothermal method for effective electrochemical hydrogen evolution reaction (HER).

1.4.2 Specific Objective

- To synthesize non-metal doped transition metal catalysts (Ni, Mo, and V catalysts doped with sulfur and phosphorus) using hydrothermal approaches.
- To conduct physiochemical and electrochemical characterization of the resulting catalysts.
- To investigate sulfur and phosphorus co-doping influences the HER performance of the synthesized catalyst.

1.5 Significance of the study

Ethiopia is actively pursuing a low-carbon, climate-resilient development pathway, as outlined in its Climate Resilient Green Economy (CRGE) strategy. A central component of this strategy is the expansion of renewable energy to reduce greenhouse gas emissions while addressing the country's growing energy demands. Despite vast renewable energy potential, particularly in hydropower, solar and wind, their intermittency poses a significant challenge to maintaining a stable and reliable energy supply. This underscores the need for efficient and scalable energy storage solutions that can conserve excess energy during periods of low demand and release it during shortages. Green hydrogen, produced via water electrolysis using surplus renewable electricity, is emerging as a crucial enabler in bridging this supply-demand gap. It not only enhances energy system flexibility and grid stability but also serves as a clean energy carrier for sectors that are hard to decarbonize, such as transportation and

industry. In this context, alkaline water electrolysis (AWE) stands out as a practical and scalable method for hydrogen production. However, the limited availability of platinum-group metal (PGM) catalysts used in conventional AWE systems presents a significant barrier.

This study contributes to green hydrogen production by developing and evaluating a non-noble metal based electrocatalyst—a sulfur- and phosphorus doped (Ni, Mo, V) material—synthesized via a hydrothermal method. The use of earth-abundant transition metals aims to replace PGMs while maintaining high catalytic activity in alkaline media. This approach aligns with national and international priorities by supporting Ethiopia's energy independence, promoting local innovation, and contributing to sustainable economic growth and job creation.

1.6 Scope of the study

The scope of this research focused on

- The synthesis and characterization of transition metal based electrocatalyst for AWE.
- Investigate the effect of synergy on the intrinsic activity and stability of the material.

The scope of this research will not focus on

- Investigate the mechanism behind alkaline water electrolysis.
- Optimization of the operation condition for alkaline water electrolysis.

1.7 Limitation of the study

Despite meaningful insights offered by this study into the electrocatalytic behavior of hydrothermally synthesized (Ni, Mo, V)-P, S catalyst in alkaline media, certain limitations should be acknowledged. Although the electrocatalyst displayed stable performance, long-term stability testing was quite limited due to restricted access to the potentiostat, which was shared among multiple researchers, as a result, extended continuous operation over several days could not be performed.

1.8 Organization of the thesis

The thesis is organized through five chapters. This chapter explores the research area using a deductive approach, progressing from a broad and general perspective to a more specific and focused discussion. The problem statement is presented from global, national and academic viewpoints, highlighting the research gap regarding economic feasibility and accessibility. The objectives of the study are clearly outlined, and its significance is articulated in the context of both global and national communities. Chapter Two presents a comprehensive literature reviews on the global energy transition, examining its current status, opportunities, and challenges, as well as their implications to Ethiopia. Additionally, the chapter discusses the potential of green hydrogen, highlighting its opportunities and challenges. Furthermore, it provides overview of water electrolysis and its different types, along with a comparative analysis of noble and transition metal-based electrocatalysts.

Chapter Three details the materials utilized in the experimental work, along with the procedures and methods applied in the research. It outlines the physiochemical and electrochemical characterization techniques, explaining their purpose and relevance to the study. Chapter Four presents the results and discussion, analyzing the physiochemical characterization findings and their interpretation, particularly in relation to XRD, SEM and XPS analysis. The chapter also evaluates the electrocatalyst's performance based on the electrochemical characterization techniques, including LSV, EIS, tafel slope and constant voltage. Furthermore, the results are compared with existing reports on noble and non-noble metal-based electrocatalysts to highlight performance improvements. Finally, conclusion and recommendation presents the conclusions drawn from the research findings and provides recommendation based on the challenges and opportunities encountered during the study.

CHAPTER TWO
LITERATURE REVIEW

2.1 Introduction

The rising global demand for energy and growing awareness about the adverse environmental consequences associated with conventional fossil energy sources have created a pressing demand for a shift toward sustainable and clean energy sources (Alex Martinos, 2025). Despite significant technological advancement in solar and wind energies, the inherent nature of intermittence of these renewable energies demands an equally developed set of efficient energy storage and energy conversion technologies. Green hydrogen produced through water electrolysis is regarded as a crucial clean energy vector capable of decarbonize and as a result, thus, harbor a set of opportunities toward the sustainable energy future (Fan et al., 2025). Being versatile, it finds applications in transport, industrial processes, and power generation and is therefore an important factor in achieving global goals for decarbonization.

Water electrolysis refers to the method of employing electricity to decompose water in to its hydrogen and oxygen components. This technique is going to be among the prime methods used to produce H_2 gas derived from renewable energy sources (Fan et al., 2025). Between the two electrochemical steps involved in electrolysis of water splitting, cathodic HER has a high significance toward determining the complete overall effectiveness of the system. However, reaction rates in HER are often sluggish due to the need for electrocatalysts to reduce energy barriers and improve the speed of reaction. It is, therefore, imperative to develop electrocatalysts of very high efficiency and affordability that are durable as well as to overcome the kinetic limitations posed by HER so those sustainable hydrogen generations become cost-effective and scalable.

This literature review seeks to outline the present state of the energy landscape as well as the ongoing worldwide shift toward cleaner and carbon-reduced energy options. The forthcoming emerging green hydrogen market is going to be explored while evaluating this sector’s potential to enhance a foundation for the decarbonization of various sectors. This study will specifically focus on hydrogen production by water electrolysis, with Particular emphasis is placed on the reaction mechanism occurring

in alkaline water electrolysis systems. This review will also cover electrocatalyst advances regarding HER, ranging from the latest high-end noble metal catalysts to low-cost transition metal-based substitutes. In addition, it will present the most important and common in-situ and ex-situ characterization techniques that are commonly applied for the purpose of study of catalyst structure, composition, and electrochemical performance. Finally, the review will point out the existing difficulties, research gaps, and future perspectives in the field to allow for an all-encompassing view of the material systems under investigation and their role in enabling efficient and scalable hydrogen production.

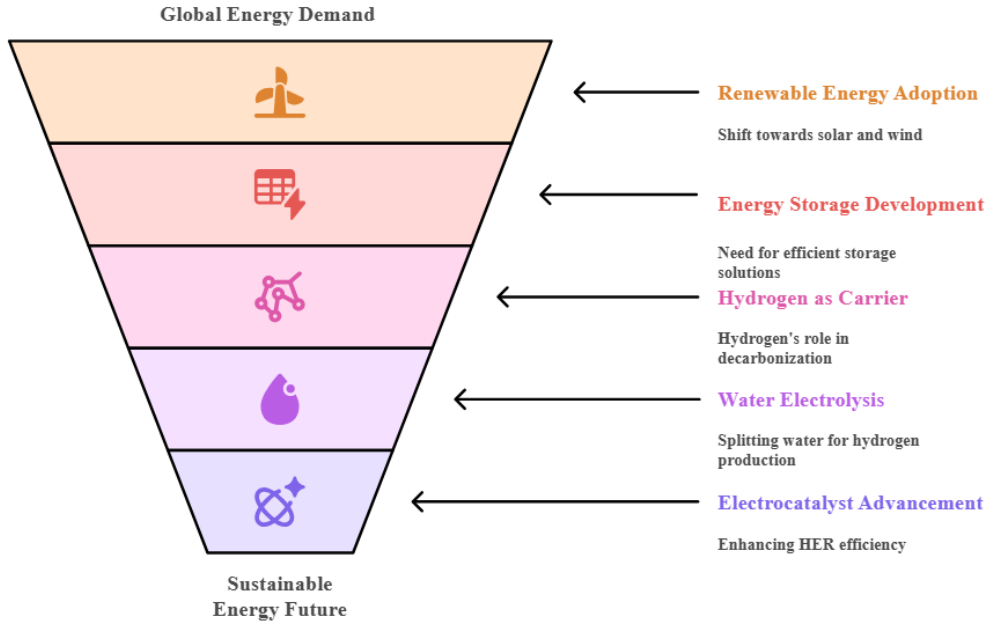

Figure 2. 1: Visual Chapter Outline

2.2 Global Energy Landscape and the History of Energy Transition

Energy transitions encompass changes in the processes, locations, and stakeholders involved in the extraction, generation, conversion, distribution, acquisition, and utilization of energy. These changes can occur across various levels, including international, regional, national, community, or industry-specific scopes (Pearson, 2018). Such transformations have resulted in the production of significantly larger and improved fuel types, the emergence of innovative technologies, as well as new usages along with behavior. Great energy transitions indeed happen through centuries - sometimes times have been referred to grand energy transitions (Pearson, 2018). The

history of energy uses has gradually seen a shift from animal labor and traditional biomass sources, like wood and agricultural wastes, which were dominant until the middle of the 19th century, to fossil fuels like coal, oil, and gas-an accelerated process that started with the Industrial Revolution to the current stage of energy transition which is shifting away from carbon-intensive sources such as petroleum and coal, towards cleaner energy options like natural gas, wind energy, solar power, and hydroelectricity. Although new energy sources surely will have dominance in due course, this transformation is generally accompanied by overlapping, sometimes lengthy, processes of adaptation. Hence, the existing energy systems and associated technologies often develop at significantly slower pace compared to half a generation ago; yet still hold a considerable foothold long after the ascendance of the new energy source(s) (Pearson, 2018). The most recent changes that have been taking place in the energy landscape seem to build up the trend of ever-increasing momentum towards the adoption of renewable energy on the global front (Alex Martinos, 2025). As observed from the 2024 data, renewables represented the greatest proportion in meeting rising worldwide energy demand, accompanied by record growth in installed renewable power capacity (Alex Martinos, 2025). By the year 2023, renewable sources contributed a significant share to the global electricity, heat, and fuels, with the sector witnessing investments to new levels, exceeding all-time records in this area (Hassan et al., 2024). Nevertheless, it is essential to acknowledge that the wide prevalence of the use of fossil fuels is still there with its substantial component in the global energy supply (Bhutada, 2022).

The most recent data as shown in Figure 2.2 show global energy consumption demand grew at an above-average pace during 2024, which translates into increased rising need across diverse energy sources such as fossil fuels, renewable energy, and nuclear power (Alex Martinos, 2025). “The power sector led this development, with demand for electricity growing almost twice as fast as wider energy demand, owing to higher demand for cooling; rising consumption by industry; transport electrification; as well as the growth of data centers and AI” (Alex Martinos, 2025).

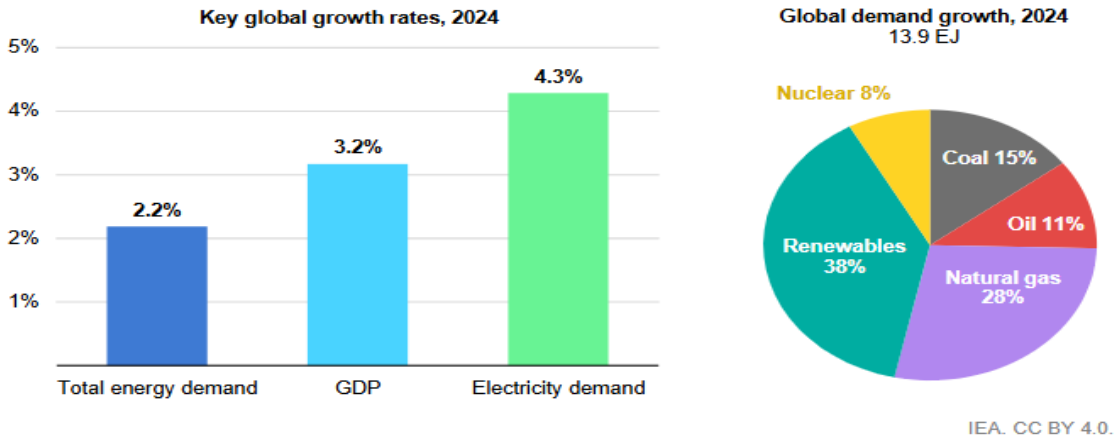

Figure 2. 2: Key worldwide expansion trends and contributions to energy consumption by type in 2024 (Alex Martinos, 2025)

2.3 Ethiopia's Renewable Energy Landscape: Progress and Potential

African nations are highly susceptible to the negative consequences brought on by climate change. The renewable energy transition has synergies with both sustainable development goals as well as global climate agreements such as the Paris Agreement. Carbon emission reductions and cleaner forms of energy, among others, allow Africa to contribute to global climate action while furthering resilience and sustainability in the economies (Ghosn et al., 2024). Renewable capacity has been increasing throughout Sub-Saharan Africa; however, the area still lags behind what its resources can achieve and the level of electrification that is needed (Yasmina Abdelilah et al., 2025). One example is Ethiopia, a Sub-Saharan country, with a wide range of renewable resource potential. Table 2.1 provides information on the usable potential of different types of energy resources in Ethiopia.

Table 2. 1: Domestic renewable energy source potentials and consumption status (Guta & Börner, 2017; Khan & Singh, 2017; G. A. Tiruye et al., 2021)

No.	Resource	Unit	Potential	Exploited
1	Hydropower	MW	45,000	< 10%
2	Solar	KWh/m^2/day	5-6	< 1%
3	Wind	MW	10,000	< 1%

4	Geothermal	MW	10,000	< 1%
5	Agricultural waste	Million tone	15-20	< 30%

The energy system of Ethiopia has not expanded parallel to the economic growth of the country, nor with the high urbanization rate and upcoming energy demand. Ethiopia's electricity demand by various sectors would rise exponentially as well. As indicated by Figure 5, electricity demand in industry and domestic sectors would rise by 46% and 18%, respectively.

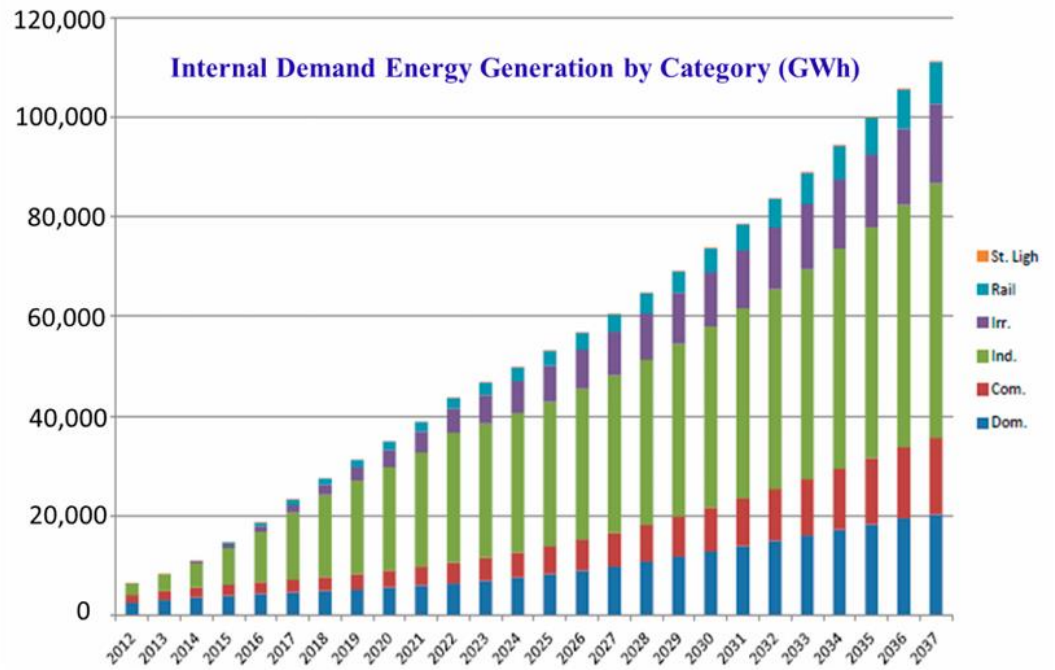

Figure 2. 3: Ethiopian energy demand forecast (G. Tiruye et al., 2021)

The renewable energy transition avails a number of major opportunities to Ethiopia in line with making use of its unexploited huge renewable resource potential for its increasing energy demand, especially in industry and transport sectors. Ethiopia faces a great challenge in making modern energy available to its population as a big percentage of that population, in particular, the ones in rural areas, are without any electricity. Renewable energy transition opens the possibility for increasing the national electrification rate towards achieving universal access by 2030. “Off-grid solar photovoltaic systems, minigrid using wind and solar, micro-hydro projects, and more are examples of decentralized renewable energy solutions to reach remote areas

where grid extension is difficult and expensive" (Tiruye et al., 2021). Ethiopia holds huge and various types of renewable energy assets including good hydropower potential (with estimates at 45000 MW), generous wind energy potential (with estimates at around 10000 MW), reputable geothermal resources (with estimates at around 5000 MW), and considerable solar irradiation. These developments enable Ethiopia to employ the indigenous means to sustain the growing energy demand. Currently, hydropower is the dominant source in the electricity mix, whereas concerted efforts are being made to develop and integrate other renewables to diversify the energy supply (Guta & Börner, 2017).

Ethiopia exhibits keen attention on green economic growth. Among other things, the shift to renewable energy will be the focus according to its Climate Resilient Green Economy (CRGE), aiming at achieving a carbon-neutral growth through this. Renewable energy generation will enhance the country's standing in reducing greenhouse gas emissions along global efforts for combating climate change (Guta & Börner, 2017). Renewable energy deployment can create conditions for technological innovations and the development of local talent and technical capacity within the energy sector. While this time is beset with technical and human capacity impediments, government policies can support innovation through R&D and skills development. There are also opportunities for local manufacturing of renewable energy technologies and accessories, which would also benefit the economy and create jobs (Tiruye et al., 2021).

Ethiopia has shown a strong dedication to renewable energy development and possesses considerable capability to draw both local and international private sector funding into its energy industry. Liberalizing the electricity sector and offering supportive incentives for renewable energy advancements will further encourage such investments. The renewable energy transition represents for Ethiopia a watershed opportunity to resolve its energy deficit, drive sustainable economic growth, achieve energy security, combat climate change, and, significantly, provide access clean energy for its citizens. With proper promotion of its large renewable resources and supportive policy measures, Ethiopia could position itself strategically at the heart of regional renewable energy (Guta & Börner, 2017).

However, as much as advancement has been made globally in the process of transitioning, it still has considerable bumps in the road, the unpredictable nature of clean energy sources, especially wind and solar, poses a significant obstacle to having consistent energy output. To fill the gap between fluctuating renewable production and stable energy demand, effective energy storage solutions are essential. Storage technologies are crucial for the conservation and use of power during periods of high renewable production for later use during the periods of high demand when production has waned. They deal with the intermittency in clean power generation by aiding greater integration of solar and wind-based power. Better energy storage systems offer enhanced grid stability, reliability, and energy system efficiency (Mikulčić et al., 2021). Energy storage improvements can make the grids stable and reliable and increase the efficiency of energy systems. Not only can we store energy for continuity of operations during insufficient or no solar energy availability, but excess energy can also be stored (Ibekwe et al., 2024).

2.4 The Role of Green Hydrogen in Advancing the Renewable Energy Economy

A green hydrogen economy means a future in which hydrogen generated from renewable sources plays a key part in cutting carbon emissions across various sectors of the global market (Hydrogen, 2025). Green hydrogen can substitute fossil fuels in uses such as powering vehicles and fueling industrial operations to create massive cuts in petroleum-related greenhouse gas emissions. Green hydrogen holds great promise as a “final step” approach for the decarbonization of challenging sectors where using electricity directly may not be feasible or could be too costly (Hydrogen, 2025). The potentials for green hydrogen are far-reaching and endless in different fields. In addition to being an energy carrier and storage medium, green hydrogen can therefore stabilize the grid by storing surplus energy from renewables when there are low demands and return the supply when there is demand. Moreover, this can be directly used in fuel cells or turbines to produce clean power (Singh, 2025).

There are multiple challenges to the mass acceptance of a green hydrogen economy. At present, generating green hydrogen—particularly through the electrolysis of water powered by renewable sources—incurs greater costs compared to hydrogen derived

from fossil fuels. Another challenge that is equally important is in the creation of sufficient infrastructure to support the handling, movement, and delivery of hydrogen. Moreover, the need for regulatory policies is felt to facilitate the green hydrogen market set up in the establishments. In addition, these obstacles represent a great deal of chances for technological innovation, economy development in the creation of industry and job opportunities (Hydrogen, 2025). Considerable growth is expected in the worldwide market of green hydrogen over the years to come because of the general realization of the value it adds as a key enabler for achieving a decarbonized future. “With the current policy landscape, demand for low-emissions hydrogen could grow ten-fold by 2030, reaching more than 6 Mtpa. While this would represent significant progress compared with today, it is a far cry from the 65 Mtpa needed by 2030 in the NZE Scenario” (Giovanni Andrean et al., 2025).

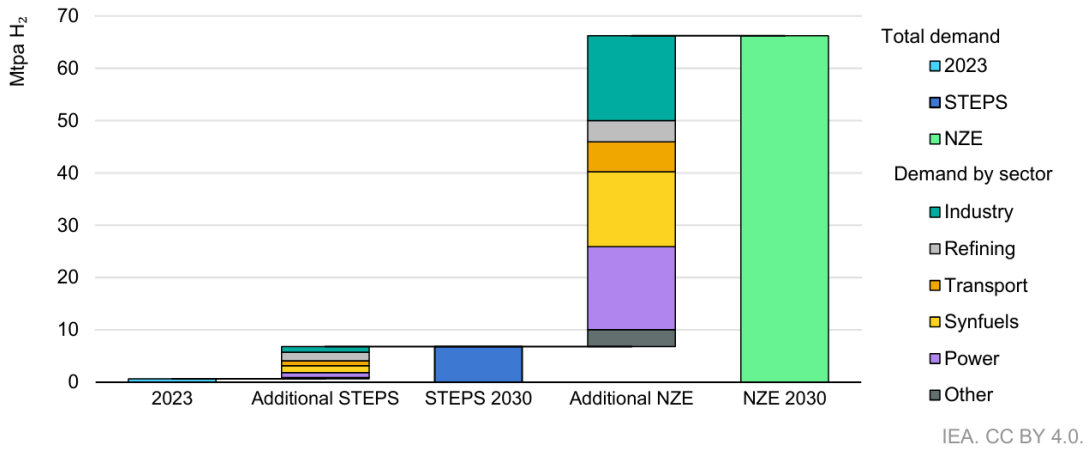

Notes: NZE = Net Zero Emissions by 2050 Scenario. STEPS = Stated Policies Scenario. “Other” includes buildings and biofuels upgrading.

Figure 2. 4: Demand for hydrogen per sector in 2023, the Stated Policies Scenario, and the 2030 Net Zero Emissions by 2050 Scenario (Giovanni Andrean et al., 2025)

2.5 Green Hydrogen Production via Water Electrolysis

Water electrolysis is a widely recognized method for hydrogen generation by splitting the water molecules using electricity. The electrolysis process may be broadly grouped into various categories depending on the electrolyte used: such as alkaline water electrolysis (AWE), proton exchange membrane (PEM) electrolysis, solid oxide electrolysis (SOEC), and anion exchange membrane (AEM) electrolysis. Among these, alkaline water electrolysis is a well-developed method that has been applied for many years (Schneider et al., 2024).

2.5.1 Alkaline Water Electrolysis (AWE)

In AWE, electrochemical reactions take place within a basic electrolyte, typically a mixture containing potassium hydroxide (KOH). At the cathode, water molecules undergo reduction, gaining electrons during the reaction and generating hydrogen gas and hydroxide ions (OH^-) (Zoulias et al., 2004). It consists of many elementary processes like the Volmer step, in which water attaches to the catalyst's surface and splits when it accepts an electron, producing adsorbed hydrogen (H*) and a hydroxide ion (Shi et al., 2025). Then, the hydrogen that has been adsorbed starts desorbing to form hydrogen gas as a consequence of the electrochemical Heyrovsky step or by means of the chemical Tafel step (Shi et al., 2025). Hydroxide ions are simultaneously oxidized at the anode, releasing electrons to generate oxygen and water during the reaction (Zoulias et al., 2004). The alkaline electrolyte facilitates the movement of hydroxide ions through the electrodes and preserves electrical conductivity while supporting the electrolysis process (Vinodh et al., 2024).

There are a number of benefits offered by AWE that make it an attractive technology for green hydrogen production (Schneider et al., 2024). It has the enormous advantage that one can use non-PGM catalysts, that is, materials based on nickel and cobalt, for both the HER and oxygen evolution reaction (OER) (Vinodh et al., 2024). It reduces the cost significantly compared to PEM electrolysis, which frequently makes use of quite expensive platinum group metals (Sebbahi et al., 2024). Operation at relatively low temperatures (typically at 40°C-90°C) results in decreased energy consumption and material damage due to elevated temperatures (Vinodh et al., 2024). Moreover, the AWE technology is mature and technologically well established, with a high level of readiness and applicability for large-scale hydrogen production purposes (Schneider et al., 2024). “The possibility of AWE to work fine with less cleaner water sources also increases the practical suitability for a wide range of settings” (Sebbahi et al., 2024).

2.5.2 Acidic (PEM) Water Electrolysis

PEM water electrolysis represents yet another major technology for hydrogen generation, using an electrolyte in the form of a solid polymer membrane that conducts protons (H^+) (Vinodh et al., 2024). PEM electrolysis takes place in an acidic environment. Water, from the anode, was oxidized to get oxygen, electrons, and

protons. These protons are then led from the membrane which serves as the proton carrier to the cathode. Here they are combined with electrons, thus producing hydrogen gas (Vinodh et al., 2024).

Compared to AWE, PEM electrolysis offers higher power densities, achieves higher output hydrogen pressures, and operates faster (Pepe et al., 2023). Electrolyte in the form of caustic liquid is also eliminated, thus minimizing safety hazards. However, in general, PEM electrolysis requires the uses of platinum-group metal catalysts, especially iridium for the OER at anode, which tends to add significantly to the capital cost base (Sebbahi et al., 2024). Despite the ongoing developments in reducing the loading of precious metals, their high cost is a major constraint for their large-scale acceptance (Araújo et al., 2024). Further, despite its potential, market penetration for PEMWE technology is still significantly lower than in the AWE market (C. R. Wang et al., 2025). Where AWE is fortunate to work with non-noble metal catalysts, PEM electrolysis needs corrosive and often expensive materials because of the acidic environment in which it operates. While PEM electrolysis can result in higher efficiencies and greater hydrogen purities, the more costly and high operating costs primarily due to the usage of noble metals, make AWE relatively cheaper, especially for large-scale applications where non-noble metal catalysis can be effectively exploited (Sebbahi et al., 2024).

2.6 Fundamental Mechanisms in Alkaline Water Electrolysis and the Hydrogen Evolution Reaction (HER)

2.6.1 Basic Mechanism of Alkaline Water Electrolysis

The general chemical reaction for alkaline water electrolysis can be written as follows:

$$2\ H_2O\ (l) \rightarrow 2H_2\ (g) + O_2(g) \qquad (2.\ 1)$$

In this process, an alkaline electrolyte such as potassium hydroxide (KOH) is really significant. An alkaline solution increases the concentration of hydroxide ions (OH^-), which carry charge between electrodes, the whole process requiring these ions to facilitate the electrochemical reactions by migrating through the electrolyte in a way to sustain conductivity in the solution (Vinodh et al., 2024).

At the anode, oxygen evolution reaction (OER) occurs, hydroxide ions lose electrons to form oxygen gas and water:

$$4OH^- (aq) \rightarrow O_2 (g) + 2H_2O (l) + 4e^- \quad (2.\ 2)$$

While at the cathode, hydrogen evolution reaction (HER) produces hydrogen gas and hydroxide ions as water molecules gain electrons:

$$2\ H_2O (l) + 2e^- \rightarrow H_2 (g) + 2OH^- (aq) \quad (2.\ 3)$$

The overall efficiency of alkaline water electrolysis depends heavily on the kinetics of OER and HER, with OER normally being the rate-limiting step because of its more complex four-electron-transfer mechanism and sluggish kinetics (You & Qiao, 2021). The development of worthy electrocatalysts for both reactions is, therefore, imperative for advancing the performances and saving energy for their implementation in alkaline water electrolyzers.

2.6.2 Detailed Electrochemical Steps of the Hydrogen Evolution Reaction (HER) in Alkaline Media

The hydrogen evolution reaction in alkaline media occurs through various electrochemical steps at the surface of the cathode catalysts (Shi et al., 2025). These steps precisely involve the adsorption of reactants, charge transfer, and desorption of products. Generally, the accepted mechanism occurs with the following steps:

1. **Volmer Step (Water Adsorption and Dissociation):** The first step involves adsorption of water molecules at the active sites of the electrocatalyst surface (Y. Zhu et al., 2024). After adsorption, the water molecule reacts with an electron from the electrode and dissociates into an adsorbed hydrogen atom (H*) and hydroxide ion (OH^-) close to the active site (Shi et al., 2025). This step can be represented as:

$$H_2O + e^- + * \rightarrow H^* + OH^- \quad (2.\ 4)$$

*denotes an active site on the catalyst surface (Y. Zhu et al., 2024).

2. **Heyrovsky or Tafel Step (Hydrogen Desorption):** The next step is to release

the adsorbed hydrogen atom H* from the catalyst surface to obtain hydrogen gas H_2. This desorption step could take place through two possible routes:

- **Heyrovsky Step (Electrochemical Desorption):** In this step, a hydrogen atom that has been adsorbed enters into a reaction with another water molecule and an electron from the electrode to produce a hydrogen molecule and hydroxide ion (Shi et al., 2025).

$$H^* + H_2O + e^- \rightarrow H_2 + OH^- + * \quad (2.5)$$

- **Tafel Step (Chemical Desorption):** Another alternative is that two hydrogen atoms adsorbed on the surface may be able to combine chemically forming a hydrogen molecule, leaving two free active sites behind (Shi et al., 2025):

$$H^* + H^* \rightarrow H_2 + 2^* \quad (2.6)$$

The overall kinetics and efficiency of the alkaline HER will depend on the extent to which the electrocatalyst surface facilitates the steps mentioned earlier (Shi et al., 2025). The catalyst would have to offer appropriate active sites for the adsorption and dissociation of water as well as hydrogen adsorption and desorption. Another crucial factor is the strength of interaction between catalyst surface and adsorbed hydrogen intermediate (H*). The optimal catalyst would thus possess a hydrogen binding energy that would allow for hydrogen gas production and release, because too strong or too weak hydrogen binding would inhibit the release of hydrogen gas (Y. Zhu et al., 2024). Besides, the electronic structure of the catalyst is an important factor that affects the processes of adsorption and desorption, which in turn have a influence on the electrocatalytic activity (Y. Zhu et al., 2024).

2.7 Electrocatalysts for Efficient HER in Alkaline Electrolysis

Electrocatalysts are key materials in numerous systems for energy transformation and retention, including fuel cells, electrolyzers, and batteries, since they promote electrochemical reactions at the electrodes' surfaces (Banoth et al., 2022). The performance of the electrocatalyst largely determines the performance and efficiency

of such technologies in minimizing the energy barrier for processes such as the hydrogen evolution reaction (HER) and the oxygen evolution reaction (OER) (Rashid et al., 2025). Water splitting is being recognized as a good choice for sustainable hydrogen production, and creating highly efficient and durable catalysts will be essential for its large-scale application (Raveendran et al., 2023). Hydrothermal synthesis is a method of making electrocatalysts that is widely in use; however, importance of exploring alternative synthesis methods is evident for the fact that given the applications and targeted properties of a material, a process might be most useful for a particular technique.

2.8 Hydrothermal Synthesis of Electrocatalysts for Enhanced HER Activity

2.8.1 Principles and Advantages of Hydrothermal Synthesis Techniques

Hydrothermal method has found widespread acceptance and is commonly used to synthesize a variety of inorganic materials, including electrocatalysts . In this method, reactions are carried out between precursors via an aqueous media, under high temperatures (usually between 100°C to 300°C) and high pressures (from 1 MPa to 100 MPa) in a closed vessel-and in this case an autoclave (Rossi et al., 2023).The very high temperatures and pressures able to enhance the solubility and reactivity of the precursors while allowing controlled nucleation and growth of crystalline materials of certain morphologies, sizes, and compositions (Fathyunes et al., 2024).

Hydrothermal synthesis presents several advantages for preparing electrocatalysts with enhanced HER activity (Fathyunes et al., 2024). Fine-tuning the property of the synthesized materials and optimizing their performance as catalyst can be done by the capacity to control very precisely the reaction parameters such as temperature, pressure, reaction time, and concentration of the precursor species (Rossi et al., 2023). Complex nanostructures can be suitably synthesized using hydrothermal methods. It permit the formation of nanowires, nanotubes, nanosheets, and hierarchical architectures, all of which provide high surface areas and expose an immense amount of active sites towards the hydrogen evolution reaction (Fathyunes et al., 2024). Moreover, hydrothermal synthesis is often a straightforward and cost-effective method which can easily be scaled in order to obtain large quantities of

electrocatalysts (Rossi et al., 2023). It also enables the synthesis of multicomponent materials and introduction of controlled doping (Jia et al., 2023).

2.8.2 Recent Applications of Hydrothermal Methods in Synthesizing HER Catalysts

There are countless examples in the recent literature that have successfully applied hydrothermal synthesis in the fabrication of efficient electrocatalysts for HER. For example, the hydrothermally synthesized NiMo catalyst showed significant HER activity in microbial electrolysis cells (Rossi et al., 2023). A bilayer electrocatalyst (NiFe/NiCo)S@NF prepared via hydrothermal means exhibited promising HER performance (Fathyunes et al., 2024). Nanotubes with nickel sulfide (Ni_3S_2) particles embedded in them, created via a combination of hydrothermal treatment and annealing, exhibited remarkable activity towards HER (P. Zhu et al., 2024). the fabrication and characterization of hierarchical NiMo-$MoO_{3-\chi}$ hollow nanotubes with excellent HER activity was put forward strategically using hydrothermal techniques (Singu et al., 2024). Hydrothermal methods were also used to produce binary and ternary metal oxide systems for water oxidation (OER). The versatility of the technique in their synthesis by using it as an approach for preparing an electrocatalyst is very well demonstrated (Bibi et al., 2025). In addition, hierarchical heterostructure electrocatalysts, precisely MoS_2@NiFeCo-Mo(doped)-LDH, have been effectively synthesized by relatively simple hydrothermal means and showed remarkable performance in overall water splitting (Moradi et al., 2024). A one-step hydrothermal method was employed to prepare phosphorus-doped MoS_2/Ni_3S_2 electrocatalysts exhibiting high activities for HER and OER (Jia et al., 2023). Given these examples, we can say that hydrothermal synthesis proved to be a powerful way to design and synthesize advanced electrocatalysts for HER.

2.9 Alternative Synthesis Methods

2.9.1 Microwave synthesis

Microwave synthesis is the process wherein chemistry can benefit from unusual conditions through direct microwave heating of reactants, thereby causing an accelerated reaction (Rashid et al., 2025). It is heating by means such as dipolar polarization or ionic conduction, wherein oscillator will cause rotation and friction by

alignment of molecules having dipoles with the oscillating microwave field, and those charged particles will do oscillatory motion and collision to produce heat. The process involves rapid heating and volumetric heating of the reaction mixture in sharp contrast to the relatively slow heating and cooling characteristics of conventional methods. An experimental description involving a microwave reactor is often used for microwave synthesis. This reactor frequently includes sealed vessels that exhibit a high temperature/pressure environment, increasing reaction rates. Precision in controlling reaction factors like temperature, pressure, and duration to modify the properties of synthesized materials accordingly. The method has been successfully employed to synthesize several electrocatalysts, including cobalt-containing compounds such as oxides, sulfides, selenides, and tellurides, which have displayed great promise for enabling both HER and OER in water-splitting processes. More examples of microwave-assisted synthesized electrocatalysts include Pt/C for ORR (Kuriganova et al., 2020), MXenes for HER (Mahabari et al., 2024), Pd-Co aerogels for ethanol oxidation (Martínez-Lázaro et al., 2023), graphene-based PtCoM (M = Mn, Ru, Mo) electrocatalysts for use in low-temperature fuel cells (Nacys et al., 2021), and nickel hydroxide nanosheets.

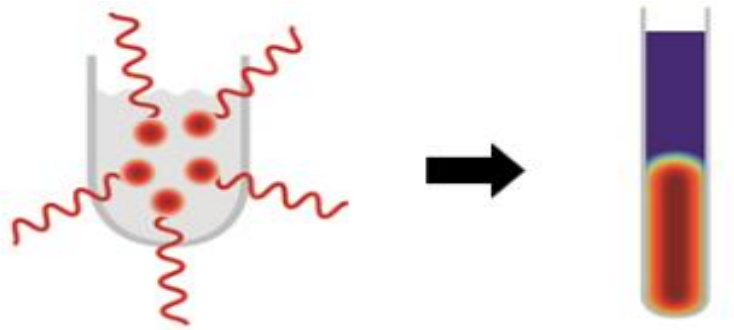

Figure 2. 5: Microwave heating (Alex Martinos, 2025)

2.9.2 Sol-Gel Method

Sol-gel technique is a liquid-phase method employed to produce both amorphous and ceramic substances (De et al., 2024). It proceeds by formation of a gel network from a colloidal solution. Typically, the process begins by dissolution in a liquid medium, such as either water or alcohol, of metal precursors like metal alkoxides or salts (De et al., 2024). The resulting solution of metal salts is hydrolyzed and condensed to produce extensive three-dimensional networks of metal-oxygen-metal bonds forming gels (Rashid et al., 2025). The gel is said to be aged in order to harden the network

after which it is subjected to drying in order to eliminate the solvent and get a porous solid called xerogel or aerogel (Esposito, 2019). This often ends by calcination at high temperatures to purposely combust any remaining organic components and initiates crystallization of material desired (Rashid et al., 2025). A number of critical steps are implemented in the experimental setup for the sol-gel technique. A precursor is initially dissolved in an appropriate liquid. A catalyst, which may be either an acid or a base, is frequently introduced in order to manipulate the rates of hydrolysis and condensation that are instrumental in shaping the final structure and characteristics of the material (De et al., 2024). After the sol is formed, it is allowed to go into gelation for a certain period of time, and gelation is usually aged in order to improve mechanical strength (Esposito, 2019). The elimination of the liquid medium from the gel occurs as a drying operation, which can be accomplished by simple evaporation, freeze-drying, or supercritical drying according to the desired porosity and texture. The last stage of soak calcination consists of subjecting the dried gel to a specific burning time under temperature conditions, where the final crystalline phase will be achieved and possible organic residues will be removed (Rashid et al., 2025). A large variety of electrocatalysts have been prepared through the sol-gel technique, including metal oxides such as TiO_2, ZrO_2, Al_2O_3, MnO_2, NiO, and Co_3O_4 (Rashid et al., 2025). It is also applied in creating perovskite materials, platinum-, Ni-, and cobalt-based electrocatalysts supported on various substrates for anion exchange membrane-based unitized regenerative fuel cells (AEM-URFCs), as shown in Figure 2.9 (Petkucheva et al., 2025), high-entropy oxides (HEOs) for water oxidation (Asim et al., 2022), and Pt-TiO2 for ORR (García-Contreras & Fernández-Valverde, 2011).

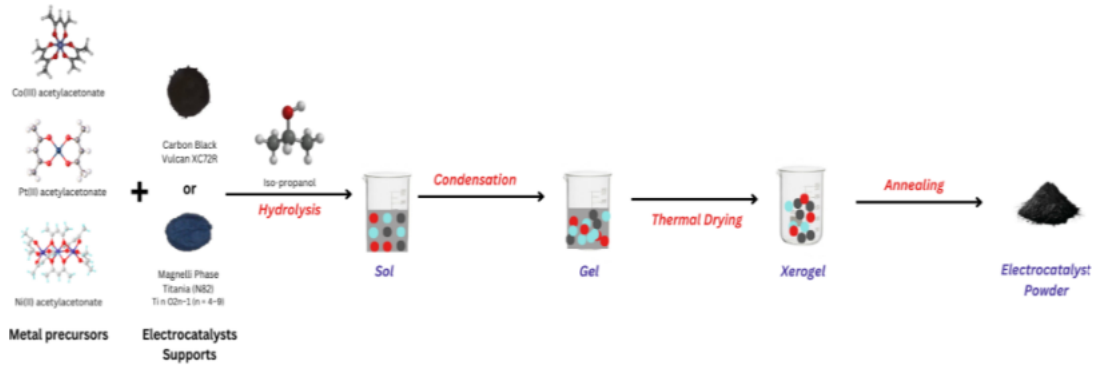

Figure 2. 6: Schematic representation of sol–gel synthesis of M1X-M2X/N82 and M1X-M2X/XC72 electrocatalysts (Petkucheva et al., 2025)

2.9.3 Electrodeposition

Electrodeposition is a method in which metal ions are reduced from an electrolyte solution onto a conductive surface using an electric potential or current (Kim et al., 2024). This process typically employs techniques such as galvanostatic (constant current), potentiostatic (constant potential), pulsed, or cyclic voltammetry to achieve precise control over metal deposition (Y. Kim et al., 2023). A standard experimental setup for electrodeposition constitutes a three-electrode electrochemical cell. This cell includes a working electrode, which is the substrate for the deposition of the electrocatalyst, a counter electrode to close the circuit, and and a reference electrode to monitor and regulate the working electrode's potential. During the process, the electrodes are immersed in the electrolyte solution containing metal ions (Miao et al., 2022). Electrolysis is carried out using a potentiostat or galvanostat, which maintains a controlled potential or current between the working and counter electrodes, enabling the reduction of metal ions onto the surface of the working electrode (Y. Kim et al., 2023). This methodology is being increasingly utilized to synthesize various electrocatalysts, such as nickel-based materials for HER and OER (Angeles-Olvera et al., 2022), high-entropy alloys, oxides, (oxy)hydroxides for water electrolysis (H.-M. Zhang et al., 2024), cobalt phosphide (Co-P) nanosphere assemblies for HER (J. Kim et al., 2023), Ni-Fe/NiO for OER (Jeon et al., 2024), copper for CO2 reduction (Bibi et al., 2025), and for noble metal-free Co-P (J. Kim et al., 2023).

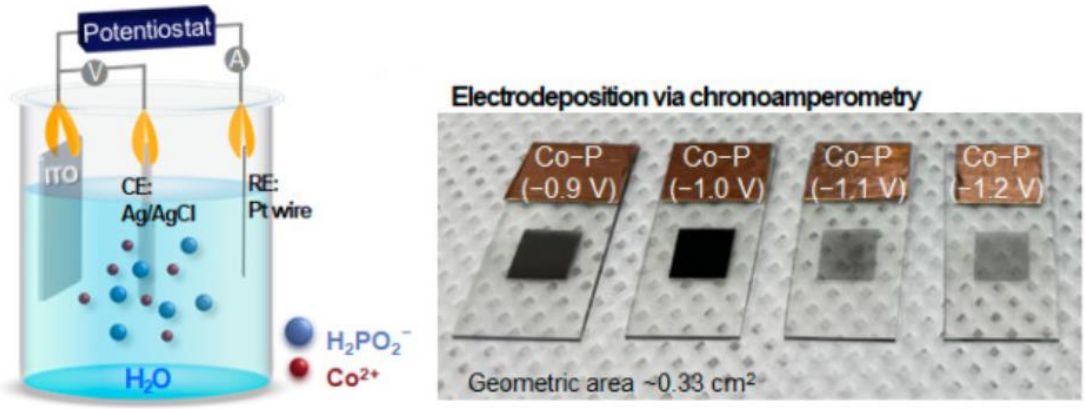

Figure 2. 7: Schematic of the Co-P nanocluster generation by electrodeposition (J. Kim et al., 2023)

2.9.4 Chemical Reduction

Chemical reduction is a synthetic technique which reduces metallic precursors like metal salts into a solvent using chemical reducing agents. Through this reduction, the

metal ions contained in the precursor solution are converted into their most elemental forms, and this process generally leads to the nucleation and growth of metal nanoparticles or other nanostructures (Banoth et al., 2022). In a routine configuration for chemical reduction, the first step is dissolving the metal precursor or precursors in a solvent such as water, alcohol, or a polyol (Kuriganova et al., 2020). Then, a chemical reducing agent is added to the solution, which may consist of sodium borohydride, ethylene glycol, ascorbic acid, or hydrazine, for starting the reduction process. The reaction mixture is typically stirred under controlled temperature for several hours so that the reactions will be completed, and the desired nanostructures formed (Kuriganova et al., 2020). The resulting electrocatalyst will then be separated from the solution, usually by filtration or centrifugation, and thoroughly washed to remove any unreacted precursor or byproducts and then dried. Annealing or heat treatment may sometimes be added as a step to further refine the properties of the electrocatalyst (Kuriganova et al., 2020). Chemical reduction has been broadly successful in preparing many types of electrocatalysts, including platinum nanoparticles for ORR and other reactions, nickel-iron catalysts for HER (Kuriganova et al., 2020), palladium-carbon catalysts for ethanol electrooxidation (Farsadrooh et al., 2020), platinum-bismuth intermetallic nanoparticles for formic acid oxidation (Roychowdhury et al., 2005), platinum-iron/carbon for glycerol electrooxidation (Lima et al., 2023), and platinum-copper/carbon for ORR and methanol electrooxidation (Pavlets et al., 2021).

Table 2. 2: Summary of alternative electrocatalyst synthesis methods

Synthesis Method	Fundamental Principles	Key Advantages	Key Disadvantages	References
Microwave Synthesis	Reactant direct heating through microwave radiation using dipolar polarization and ionic conduction.	Rapid reaction times, energy efficiency, homogeneous heating, uniform particle size, high surface	Requires specialized equipment, scalability challenges, and rigorous parameter optimization,	(Kuriganova et al., 2020; Martínez-Lázaro et al., 2023; Nacys et al., 2021;

		area.	not always feasible for reaction monitoring.	Rashid et al., 2025)
Sol-Gel Method	Formation of a gel network from a sol through hydrolysis and condensation of precursors, followed by drying and calcination.	Low processing temperatures, high homogeneity, precise control over composition and microstructure, versatile for various forms.	Slow gelation, shrinkage during drying, requires calcination (potential sintering), residual organic waste.	(Asim et al., 2022; De et al., 2024; Esposito, 2019; García-Contreras & Fernández-Valverde, 2011; Petkucheva et al., 2025; Rashid et al., 2025)
Electrodeposition	Reduction of metal ions from an electrolyte onto a conductive substrate by applying an electric potential or current.	Simple and cost-effective, precise control over thickness and morphology, direct deposition on substrate (binder-free), suitable for large scale.	Substrate influence on morphology, challenges in uniform deposition over large areas, requires parameter optimization, bubble formation	(Bibi et al., 2025; Jeon et al., 2024; Kim et al., 2024; J. Kim et al., 2023; Y. Kim et al., 2023; Miao et al., 2022; H.-M. Zhang et

			issues.	al., 2024)
Chemical Reduction	Reduction of metal precursors in a solution using a chemical reducing agent, leading to nucleation and growth of nanoparticles.	Simple procedure, low temperatures, good control over particle size and composition, suitable for various metal and alloy nanoparticles, can prepare supported catalysts.	Potential for nanoparticle agglomeration, may require capping agents, purity affected by residuals, morphology control can be challenging.	(Banoth et al., 2022; Kuriganova et al., 2020; Lima et al., 2023; Pavlets et al., 2021)

2.9.5 Emerging Electrocatalyst Synthesis Methods

There are some emerging electrocatalyst synthesis techniques gaining attention in the literature aside from the traditional ones. These methods often have their unique advantages for specific applications or systems of materials. Mechanical milling is a top-down approach that generate nanoscale materials from bulk precursors by high-energy impact, being very useful for certain nanocomposite materials (Ndlwana et al., 2021). For the production of nanofibers from a variety of materials, electrospinning usually utilizes polymers by drawing charged threads from polymer melts or solutions. Another green approach for the production of noble metal nanoparticles is by laser ablation, wherein a finely focused laser beam is directed onto a target material, vaporizing it and in turn forming nanoparticles (Altammar, 2023). Sputtering is an alternative to the expensive electron-beam lithography processes whereby some micro particles, is expelled from the surface of a solid material subject to bombardment by energetic plasma or gas particles. In the method of electron explosion, a thin metal wire is subjected to a high current pulse, which leads to its kind of explosion into nanoparticles. Ionothermal synthesis is a process that uses ionic liquids, as both solvent and reaction medium at high temperatures, and offers an exceptional medium

for the synthesis of certain materials (Ndlwana et al., 2021). Lastly, pulse laser ablation liquid synthesis (PLAL) is being investigated for controlling the surface chemical feature of nanocatalysts, thereby allowing the formulation of stabilizer-free nanoparticles tailored to display specific electrocatalytic properties (Zheng et al., 2021).

Selecting the best process of synthesis is very critical for the attainment of the optimum electrocatalytic performance. The specifications with regard to morphological and particle size consideration, composition, economics, and return would have to be considered scrupulously during synthesis. The emerging methods of synthesis, such as mechanical milling, electrospinning, laser ablation, sputtering, electron explosion, ionothermal synthesis, and pulse laser ablation in liquid synthesis, are showing that the field is alive-a vibrant one, in continued evolution. Emerging new direction in electrocatalyst synthesis that targets sustainability in and scalability of emerging methods will also integrate the multiple methods of synthesis to achieve synergistic effects and better control while using advanced characterization techniques for rational design to enable high-performing electrocatalysts towards a cleaner energy future.

2.10 State-of-the-Art Noble Metal-Based Catalysts: Performance and Limitations

Platinum (Pt) is regarded as the leading electrocatalyst for the hydrogen evolution reaction (HER) across a broad pH spectrum, including under alkaline conditions (F. Wang et al., 2025). This is due to its excellent hydrogen bonding characteristics, which support both the attachment of hydrogen intermediates and the release of hydrogen gas, thereby enabling high catalytic performance (Xie et al., 2024). Other noble metals like ruthenium (Ru) and iridium (Ir) are also known for their effective HER performance. (Solangi et al., 2024). One may find Ruthenium as promising alternatives to platinum when considering some specific applications such as that of HER (F. Wang et al., 2025). Noble metals possess great electrocatalytic activities but their large-scale use as catalysts for producing hydrogen (HER) in general is frustrated by their drawbacks. Given the high cost and low abundance of platinum, ruthenium, and iridium, these metals are not viable for large-scale water electrolysis

for hydrogen production (F. Wang et al., 2025). Additionally, under certain alkaline operating conditions, noble metal catalysts can suffer from dissolution or surface oxidation, leading to degradation of their catalytic activity over time (Li & Baek, 2019). Thus, there is a global research initiative to replace or significantly reduce the use of precious metals for the HER.

2.11 Transition Metal-Based (Non-Noble) Catalysts: An Overview of Recent Progress

To overcome the limitations linked to noble metal catalysts, there has been significant attention in exploring low-cost and naturally abundant transition metals: nickel (Ni), molybdenum (Mo), vanadium (V), iron (Fe), and cobalt (Co) and their respective compounds which may serve as cost effective alternatives for the HER in alkaline electrolytes (Fathyunes et al., 2024). As a result of these elements' inherent availability and lower economic viability, these compounds would make a more suitable choice for large-scale applications compared with other possible candidates. One of the recent developments in this field has resulted in different classes of transition HER catalysts composed of metals such as alloys, oxides, hydroxides, sulfides, phosphide compounds, nitrides, and carbide-based materials (Solangi et al., 2024).

Nickel-based materials have recently been identified as strong contenders for the overall alkaline HER process because of their inherent activity and stability in alkaline media (Fathyunes et al., 2024). Nickel foam and nickel alloys mixed with other transition elements, as well as oxides, hydroxides, phosphides, and sulfides of nickel, have shown remarkable efficiency for the HER activity (Vij et al., 2017). For instance, the combination of $Ti_3C_2T_x$ MXene into $Co(OH)_2$ has exhibited an overpotential of 380 mV at 10 $mAcm^{-2}$ on HER in alkaline conditions (Solangi et al., 2024). Nickel sulfide (Ni_3S_2) nanoparticles integrated with carbon nanotubes on nickel foam have also exhibited outstanding performance in HER with low overpotential of -87 mV at 10 $mAcm^{-2}$ (P. Zhu et al., 2024).

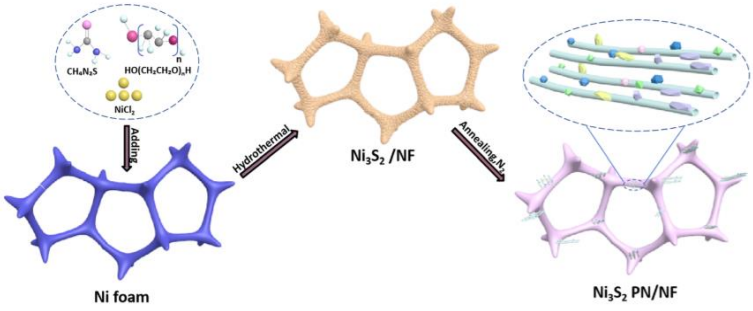

Figure 2. 8: Formation of Ni2S2 PN/NF composite (P. Zhu et al., 2024)

Molybdenum-based compounds like molybdenum sulfides, phosphides, and carbides have likewise noticed the attention of many scientists as HER electrocatalysts. Sulfur and nitrogen dual-doped molybdenum phosphides have demonstrated impressive activity for hydrogen evolution reactions in both alkaline and acid electrolytes, an overpotential of 20 mV and 49 mV at 10 $mAcm^{-2}$, respectively (Anjum & Lee, 2017). For an improved HER performance, ternary alloy catalysts, Ni-Mo-P, had also been gives an overpotential of 28 mV at 10 $mAcm^{-2}$ (Bang et al., 2022).

Many strategies have been developed in the advancement of transition metal-based HER catalysts to further enhance its performance (Fathyunes et al., 2024). By combining different transition metals in an alloy form, it results into synergistic effects leading to optimum electronic systems and hydrogen binding energies of the catalyst (Fathyunes et al., 2024). Incorporation with non-metal elements, like sulfur and phosphorus, can change electronic properties, create active sites, and improve stability (Jia et al., 2023). Enhancement of HER activity can be exerted by manipulating the nanoscale catalyst morphology, thereby creating nanostructures with high surface area and exposed active sites (X. Zhang et al., 2024). Combining various catalytic materials to form heterostructures can indeed lead to enhanced charge transfer effectiveness and increased synergistic catalytic capability (Jia et al., 2023).

2.11.1 Recent Studies on Ni-Mo-V Catalysts for Alkaline HER

Nickel-molybdenum (Ni-Mo) compounds have undergone extensive investigation owing to their promise as affordable alternatives to noble metals for catalyzing the hydrogen evolution reaction (HER) in basic media (Kamel et al., 2025). The combined effect of nickel and molybdenum improves the overall catalytic efficiency. Nickel has been shown to aid in the splitting of water, an important step in alkaline

HER, while molybdenum bears favorable hydrogen adsorption properties (Rossi et al., 2023). Studies suggest that during the HER catalysis on Ni-Mo catalysts, molybdenum species, particularly $Mo3^{+}$, play an important role as the active sites, while nickel assists by dispersing and activating molybdenum species (Bau et al., 2020). Recent studies have showed that there is great promise of almost all Ni-Mo based electrocatalysts. Hierarchical 3-D NiMo-based electrocatalysts have reached current densities close to those of top-tier Pt/C catalysts by high surface area, Figure 2.7, in alkaline conditions (Fang et al., 2016). NiMo catalyst synthesized by hydrothermal method showed negligible overpotential near Pt in microbial electrolysis cells (Rossi et al., 2023).

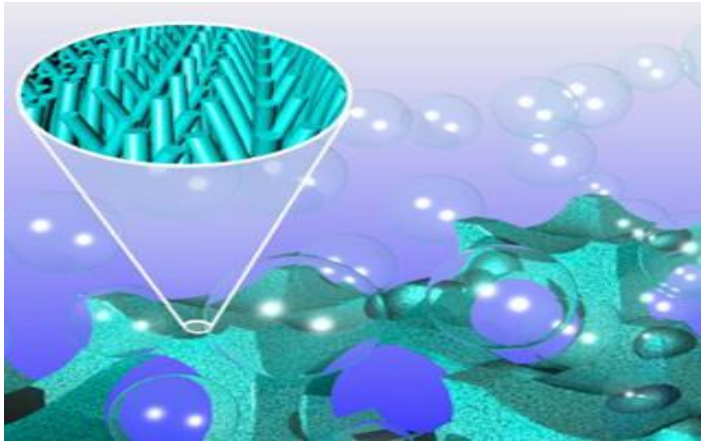

Figure 2. 9: Schematic illustration of the 3-D NiMo electrocatalyst surface (Fang et al., 2016)

Electrodeposition techniques that employ an innovative alkaline green lactate bath have been used to grow nanostructured nickel-molybdenum alloys with an outstanding molybdenum content tailored for highly effective HER (Kamel et al., 2025). Some studies have also showed instability of molybdenum in Ni-Mo alloys under alkaline conditions when dissolved and oxidized. On the other hand, they have suggested that dissolved molybdenum species can be beneficial toward promoting HER activity on other metals (Yang et al., 2024). Improving Ni-Mo catalysts with carbon supports has been investigated as a means to improve their efficiency for the alkaline HER (Patil et al., 2019). Moreover, the synthesis of hierarchical NiMo-MoO_{3-x} hollow nanotubes highly contributes toward the excellent electrocatalytic activity for hydrogen evolution with less overpotentials (Singu et al., 2024). These

outcomes collectively suggest the significant promise of Ni-Mo based materials to serve as efficient and cost-effective substitutes for noble metals in alkaline HER.

While nickel and molybdenum have been extensively investigated for alkaline HER, there has been comparatively less attention given to vanadium as a third metallic component in ternary Ni-Mo-V electrocatalysts in recent literature-which provides supporting research snippets (Vij et al., 2017). Vanadium has unique electronic and catalytic properties that could provide a very interesting boost to the properties of Ni-Mo-based catalysts. With respect to electrocatalysis, vanadium compounds have been investigated; some reports highlight that vanadium doping in other metal sulfide-based systems enhances their catalytic performance for both OER and HER (Jia et al., 2023).There is, though, a noticeable gap in the collection for direct investigation of the said ternary metallic systems of nickel-molybdenum-vanadium with respect to the reaction seeking hydrogen evolution in alkaline media. This indicates that the investigation of the Ni-Mo-V ternary system for alkaline HER is a relatively less-explored area with key prospects for breakthroughs and innovations.

It may be proposed that with the already established advantages of Ni-Mo binary systems and the potentiality of vanadium as a dopant with other catalytic materials, the incorporation of vanadium as a dopant into a Ni-Mo matrix would lead to further improvement in facilitating HER. This means that vanadium could introduce some synergistic effects by modifying the electronic configuration of the catalyst and optimizing the interaction strength of hydrogen into a range acceptable for good adsorption and desorption. In addition, the presence of vanadium promotes the creation of a greater number of reactive sites or probably alter the surface characteristics for water dissociation in alkaline HER. The coupling of these three distinct transition metals featuring different electronic properties would create a ternary system possessing superior reaction efficiency and durability over the Ni-Mo binary system. Further work focusing on the specific fabrication and investigation of Ni-Mo-V ternary electrocatalysts will be pertinent in confirming these assumptions and exploring the system fully for efficient hydrogen production.

2.12 In-situ and Ex-situ Characterization Techniques for Analyzing HER Electrocatalysts

2.12.1 Common Ex-situ Techniques for Structural and Morphological Analysis

Several external techniques are routinely adopted to perform the ex situ characterization of structural and morphological properties of electrocatalysts before and after electrochemical tests (Fathyunes et al., 2024). X-ray diffraction (XRD) is an accurate mode of characterizing the arrangement of atoms in the lattice, phase makeup, and size of crystalline domains of catalysts and, through a careful analysis of the intensity diffraction patterns, it can be determined whether specific metal phases, oxides, sulfides, or phosphides exist in the synthesized electrocatalysts. On the other hand, Scanning Electron Microscopy (SEM) and Transmission Electron Microscopy (TEM) are vital techniques used to analyze of the catalyst's morphology, particle size, and microstructure (Fathyunes et al., 2024). Surface morphology and particle-size distribution can be investigated using SEM, while TEM can provide higher resolution internal structure images and information on crystallinity and defects. X-ray photoelectron spectroscopy (XPS) is a technique sensitive to surface characteristics, used to derive information regarding what elements are present and the oxidation states of the elements present in the catalyst material (Kamel et al., 2025). The XPS analysis is useful in understanding the chemical state of the metal centers involved in catalysis and the amount of dopants, such as sulfur and phosphorus, on the catalyst surface.

2.12.2 Electrochemical Methods for Evaluating Catalytic Activity and Performance

Electrochemical methods are highly significant in assessing the catalytic performance of HER electrocatalysts (Kamel et al., 2025). Cyclic voltammetry (CV) is employed to investigate how the catalyst behaves electrochemically across different potentials. It provides enhanced insight into the multiple redox interactions occurring at the catalyst's surface. Linear sweep voltammetry (LSV) is primarily used in forming polarization curves: traces showing the progress of current response relative to applied voltage. These can be utilized to derive key performance numbers such as the extra voltage required for a specific current output (e.g. 10 mA cm^{-2}) and the Tafel

slope (Kamel et al., 2025). The Tafel slope offers essential insights into how the reaction proceeds and the slowest step in the HER sequence. Electrochemical impedance spectroscopy (EIS) is a robust method used to investigate how electrical charges move and to evaluate resistance at the boundary between the electrode and the electrolyte (Solangi et al., 2024). The impedance spectra contain vital information about how the reaction unfolds and how easily electric current flows through the catalyst.

2.12.3 Advanced In-situ Techniques for Understanding Reaction Mechanisms and Catalyst Evolution

Besides ex situ and standard electrochemical techniques, advanced in situ characterization are increasingly employed to gain insights into the mechanisms of the HER reaction and structural evolution of the catalyst under operating conditions (Bau et al., 2020).

In situ spectroscopies such as Raman spectroscopy, infrared (IR) spectroscopy, and in situ X-ray photoelectron spectroscopy (XPS) grant researchers the ability to probe the catalyst surface and identify reaction intermediates while the electrochemical reaction is actually occurring (Bau et al., 2020). These techniques do have the ability to provide valuable information about the chemical bonding and surface changes taking place during HER.

The in-situ advanced imaging methods, including transmission electron microscopy (TEM) and scanning tunneling microscopy (STM), allow visualizing the physical and surface-level transformations of the catalysts under HER conditions in real time (Wan et al., 2025). In-situ electrochemical liquid cell TEM has notably become an effective method for detecting catalyst rearrangements on the atomic scale under realistic reaction conditions (Wan et al., 2025).

2.13 Challenges and Future Perspectives in the Development of Efficient HER Electrocatalysts

2.13.1 Current Limitations and Bottlenecks in Non-Noble Metal Catalysis

Despite substantial progress in developing non-noble metal electrocatalysts for hydrogen evolution reaction (HER), a number of attendant limitations and bottlenecks

remain. The activity of several non-noble metal catalysts appears promising; however, their performances, particularly with respect to achieving lower overpotentials than those of noble metals such as platinum, are often found to be lacking (Vij et al., 2017). In addition to this, the major challenge at present is the long term stability of many non-noble metal catalysts under alkaline HER conditions. These catalysts have been pointed out to suffer degradation mechanisms such as electrochemical corrosion, material dissolution, and phase transformation that result in their catalytic activity being low with an increase in time.

Another key challenge lies in developing a comprehensive understanding of the structure-activity relationships in catalysts based on non-noble metals (Shen et al., 2025). Despite great efforts to relate the performance of the catalyst with its composition, morphology, and electronic properties, deeper fundamental understanding about the active sites at the atomic level and the reactions taking place at an atomic level is still required to rationally lay down the designs of more efficient catalysts. And finally, the cost-effectiveness and scaling up of high-performance non-noble metal catalysts to the level required for large-scale hydrogen production remain major concerns. It is important to develop synthesis methods that can be not only effective within the laboratory but also translated easily for scaling and becoming economically feasible for industrial applications.

2.13.2 Promising Future Research Directions for Achieving High-Performance and Durable HER Catalysts

The HER electrocatalyst presents exceptional future avenues for research in alkaline water electrolysis, and many of the paths for promising results are being actively followed (Solangi et al., 2024). As supported by computational methods and theoretical insights, rational catalyst design will start becoming a significant factor in developing electrocatalysts for the next generation of HER applications. Machine learning approaches are also emerging as powerful tools to identifying promising catalytic materials from an enormous compositional and structural space (Wu et al., 2025).

Further beyond conventional transition metal oxides, sulfides, and phosphides, exploring new materials and structures remains a promising way forward. MXenes, high-entropy alloys, and other novel compounds with exotic electronic and structural

properties are researched for catalytic endowment as high-efficiency HER catalysts (Solangi et al., 2024). It will further aim formulating nanostructures with the desired morphology, such as hierarchical structures, core-shell architectures, and porous materials to increase surface area exposure and active sites.

The advanced in-situ characterisation techniques will be extremely beneficial to describe the reaction mechanisms and understand the dynamic alterations of surfaces of catalyst occurring during operational conditions (Shen et al., 2025). The rational design of enhanced and durable catalysts will significantly benefit from the insights generated. Another major thrust of research will focus on the stability of non-noble metal catalysts. This includes investigations into surface protection techniques, self-healing catalysts, and optimization of operating conditions to reduce degradation (Yang et al., 2024). Finally, the following doping or co-doping strategies involving sulfur and phosphorous will continue to study effective methods of tuning electronic attributions as well as structural properties in electrocatalysts and thereby improving the HER performance of such materials (Bang et al., 2022).

CHAPTER THREE
MATERIALS AND METHODS

3.1 Chemicals and Materials

3.1.1 Chemicals

In the present work, the following analytical grade reagents were used during the experiment. Nickel foam (NF, purity > 99.9%; and thickness 5 mm) as substrate, Nickel acetate tetra hydrate **(**$Ni(CH_3COO)_2.4H_2O$ 98%, Loba Chemie, Mumbai, India**)**, Ammonium molybdate tetra hydrate **(**$(NH_4)_6MO_7O_{24}.4H_2O$ 99.3%, Loba Chemie, Mumbai, India**)**, Sodium ortho vanadate **(**Na_3VO_4 99 %, Central Drug House, New Delhi, India**)**, Urea (NH_2CONH_2 99.5 %, Central Drug House, New Delhi, India), Sodium hypophosphite **(**NaH_2PO_2 99 %, Guangdong Guanghua Sci-Tech, Guangdong, China**),** Sodium pyro sulfite ($Na_2S_2O_5$ 96 %, Guangdong Guanghua Sci-Tech, Guangdong, China), Potassium hydroxide (KOH 85 %, Central Drug House, New Delhi, India), Hydrochloric acid (HCl), Ethanol and Deionized water.

3.1.2 Equipments

The equipment and apparatus utilized in this research, along with their respective purposes, are summarized in Table 3.1 below.

Table 3. 1: Equipment and apparatus used during the study

Equipment/Apparatus	Purpose
Digital Balance	For accurately weighing chemicals and materials
Spatula	For transferring and handling solid reagents
Aluminum Foil	For covering and sealing vessels during synthesis
Beaker	For preparing and mixing solutions
Magnetic Stirrer	For homogeneous mixing of precursor solutions
Autoclave	For hydrothermal synthesis under controlled temperature
Oven	For hydrothermal synthesis and drying the synthesized material
Ultrasonicator	For dispersing materials and cleaning substrates
XRD	For examining the crystallinity of the material

SEM	For analyzing surface morphology of the catalyst
XPS	For determining surface elemental composition and chemical states
SP-300 Potentiostat	For electrochemical measurements(e.g., LSV, EIS, Cst V)

3.2 Experimental Design

3.2.1 Design Strategy of (Ni, Mo, V)-P, S Electrocatalysts

In this study, a hydrothermal synthesis method was employed to fabricate (Ni, Mo, V)-P, S-based electrocatalysts supported on nickel foam substrates. The experimental design primarily focused on anionic regulation through controlled variation of precursor concentrations for the non-metal dopants, phosphorus (P) and sulfur (S), aiming to achieve improved HER activity. Other pretreatment and synthesis parameters—including acidic cleaning condition, reaction temperature, time, and pH—was held constant throughout the study to isolate the effects of elemental composition on the electrocatalytic performance.

The synthesis was conducted in a Teflon-lined stainless steel autoclave at 150 °C for 12 hours under mildly alkaline conditions using nickel foam, pretreated with 3M HCl, as a substrate. These conditions were selected based on established procedures reported in previous literature (Ha et al., 2023) to support controlled doping, nanostructure formation, and homogeneous phase development. A univariate optimization strategy was implemented, where the concentration of one precursor was varied over a defined range while maintaining the others at fixed baseline values. This method allowed for the evaluation of the individual contribution of each element to the overall catalytic performance toward the hydrogen evolution reaction (HER). The optimal concentration for each element was determined based on electrochemical performance metrics, overpotential at a current density of 10 mA cm^{-2} and maximum current density.

Table 3. 2: Concentration matrix used during anionic regulation

Element	Chemical Precursor	Concentration Range (mmol)	Step Interval (M)	Optimization Technique

P	Sodium hypophosphite	0.01 – 0.15	0.05	Univariate
S	Sodium Pyrosulfite	0.1 – 0.25	0.05	Univariate

Each catalyst formulation was synthesized, washed, dried, and subjected to electrochemical characterization in 1 M KOH electrolyte. The catalyst with the low overpotential was selected as the optimal composition.

3.2.2 Hydrothermal Synthesis of (Ni, Mo, V)-P, S electrocatalyst

The (Ni, Mo, V)-P, S electrocatalyst grown on the Nickel foam (NF) was prepared by a single step hydrothermal method. The procedure consisted of two main stages: (1) Pre-treatment of the nickel foam substrate and (2) Preparation of the hydrothermal precursor solution.

(1) Pre-treatment of the nickel foam

To ensure good adhesion of the catalyst and eliminate surface contaminants, the nickel foam (1 × 1 cm^2) was subjected to a thorough cleaning process. Initially, in order to remove the surface oxide layer and impurities, trimmed nickel foam (NF), which is used as substrate with 1 × 1 cm^2 dimension, was pre-treated using 3 M HCl solution under ultrasonication for 20 min. This step was followed by a second ultrasonication treatment in ethanol for another 20 minutes to remove any organic residues. Finally, the NF was rinsed thoroughly with deionized water to eliminate residual solvents and acid, and then dried in a laboratory oven at 80 °C for 3 hours. This pre-treatment ensured a clean and active surface for effective nucleation and growth of the electrocatalyst during the hydrothermal process.

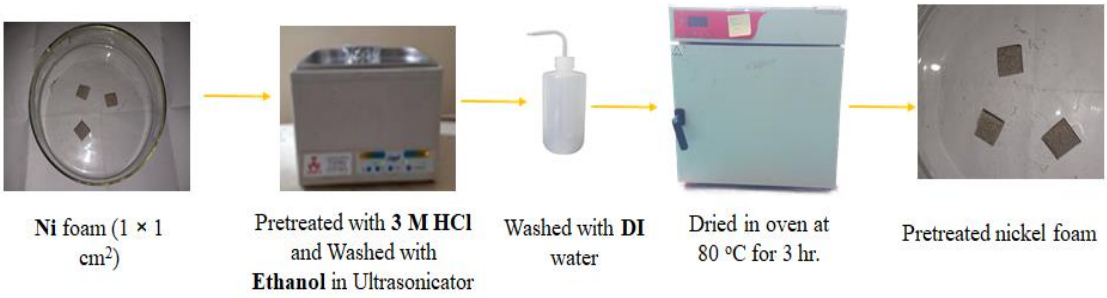

Figure 3. 1: Pretreatment of nickel foam

(2) Preparation of the hydrothermal precursor solution

The hydrothermal solution starts by dissolving 5 mmol urea CO $(NH_2)_2$ in 30 mL deionized (DI) water. The following reagents were sequentially added to the solution under continuous stirring: 0.1 mmol Sodium hypo phosphite **(**NaH_2PO_2**)**, 0.2 mmol Sodium pyrosulfite ($Na_2S_2O_5$), 0.1 mmol Ammonium molybdate tetra hydrate **(**$(NH_4)_6MO_7O_{24}.4H_2O$**)**, 1 mmol Nickel acetate tetra hydrate **(**$Ni(CH_3COO)_2.4H_2O$**)**, and 0.4 mmol Sodium orthovanadate **(**Na_3VO_4**)**. The mixture was stirred thoroughly until a homogeneous solution was formed. The pretreated nickel foam (1 × 1 cm^2) was submerged into the solution and ultrasonicated for 35 minutes precursor infiltration. Afterward, the entire mixture, including the immersed nickel foam, was transferred into a 100 mL Teflon-lined stainless-steel autoclave. The sealed autoclave was heated at 150 °C for 12 hr in an oven. Upon completion, the reactor was allowed to cool naturally to room temperature. The final product was then washed several times with DI water and ethanol to remove residual precursors, and then dried at 80 °C overnight.

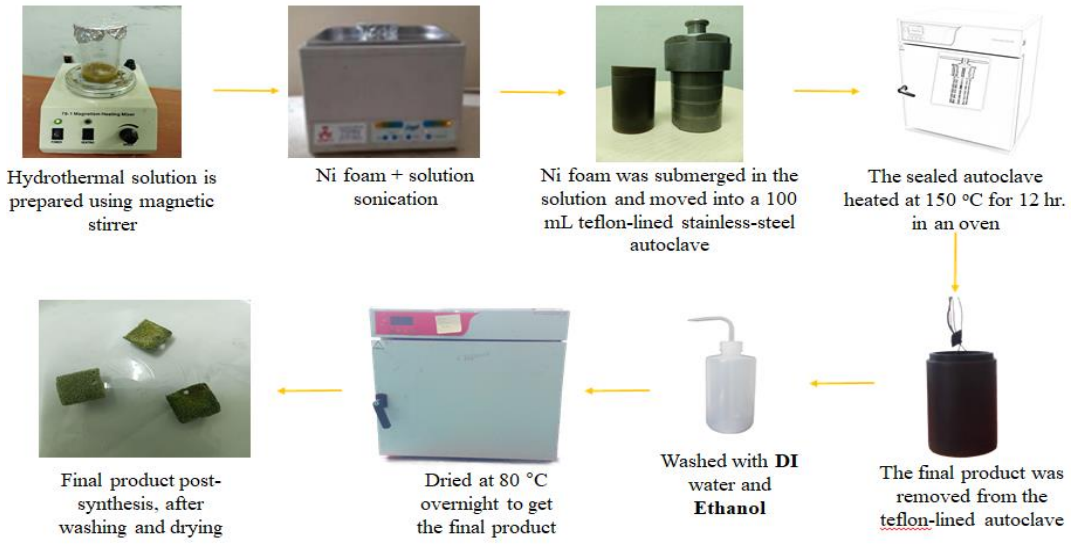

Figure 3. 2: Preparation of hydrothermal precursor solution

3.2.3 Hydrothermal Synthesis of Controlled Samples

In order to investigate each element's contribution to the structural and electrochemical features of the electrocatalyst, the different controlled samples were synthesized at the hydrothermal condition by excluding one or two dopant precursors from the full (Ni, Mo, V)-P, S composition. The controlled variants included (Ni, Mo, V)-P, made without sodium pyrosulfite ($Na_2S_2O_5$) in order to eliminate sulfur and to assess its effect; NiMoV, prepared with neither phosphorus nor sulfur by excluding sodium hypophosphite (NaH_2PO_2) and sodium pyrosulfite ($Na_2S_2O_5$), to ascertain the influence of co-doping; and NiMo, prepared without vanadium, phosphorus, and sulfur precursors (Na_3VO_4, NaH_2PO_2, $Na_2S_2O_5$) to evaluate the effect of just nickel and molybdenum. This exclusion of systematic samples allowed ruling in or ruling out a synergistic or individual role that sulfur, phosphorus, and vanadium play in HER activity.

To investigate the effect of the phosphorus, sodium hypophosphite (NaH_2PO_2), was varied at 0.01, 0.05, 0.1, and 0.15 mmol, yielding the samples NiMoVP-0.01, NiMoVP-0.05, NiMoVP-0.1, and NiMoVP-0.15, respectively. A series of sulfur-doped catalysts, designated as NiMoVPS-x, were also synthesized by varying the amount of sodium pyrosulfite ($Na_2S_2O_5$) to 0.1, 0.15, 0.2, and 0.25 mmol, respectively, in order to investigate the influence of sulfur doping concentration on the electrocatalytic performance. The resulting samples were labeled NiMoVPS-0.1, NiMoVPS-0.15, NiMoVPS-0.2, and NiMoVPS-0.25, corresponding to the respective $Na_2S_2O_5$ dosages. This variation was aimed at investigating phosphorus and sulfur incorporation and identifying the doping level that yields the most efficient hydrogen evolution activity. The HER activity of these samples was evaluated based on the overpotential required to reach a current density of 10 mA cm^{-2} and the maximum current density determined from linear sweep voltammetry measurements.

3.3 Characterization

3.3.1 Structural, Morphological and Compositional Characterization

The synthesized electrocatalyst was characterized by means of X-ray diffraction (XRD), SEM-EDS, and XPS. X-ray diffraction (XRD) was performed on a Shimadzu XRD-7000 with Cu Kα to prove the formation of crystalline phases. Based on Bragg's law, this method can reveal vital information about the crystal structure, phase

composition, and crystallinity of the materials. Using SEM/EDS, the morphology and elemental distribution were further examined with MIRA3 TESCAN SEM at an accelerating voltage of 20 kV and in secondary electron mode. SEM stands as a vital tool for investigating microstructural features such as porosity, surface roughness, and particle distribution-a-couple of characteristics directly related to HER performance. EDS, in concert with SEM, allows one to qualitatively as well as semi-quantitatively determine the composition and distribution of elements, all of which provide clues on the homogeneity of the material and the presence of elements that act as catalysts. After this, XPS with an ULVAC PHI 5000 VersaProbe III was used to evaluate the surface chemical compositions and oxidation states of the elements present. It is a surface-sensitive technique that inspects the chemical state and bonding environment of the elements on the catalyst surface.

3.3.2 Electrochemical Characterization

Electrochemical techniques are the primary collection of methods for directly measuring the performance of electrocatalysts in a way that is pertinent to their practical application (Napporn et al., 2018). The methods yield quantitative data that characterize the activity of the catalyst, the reaction kinetics, and its stability.

3.3.2.1 Linear Sweep Voltammetry (LSV)

Linear Sweep Voltammetry (LSV) is an electrochemical technique which is a form of potentiostatic technique, i.e., it fixes the potential of the working electrode. While conducting an LSV experiment, the potential sweeps in one direction linearly from a start to an end value and the resulting current is measured. An LSV experiment generates a polarization curve, i.e., a plot of current vs. potential. It is a widely used and reliable method for generating quantitative information regarding electrochemical systems. In electrocatalysis, LSV is the standard approach for quantifying the activity of the catalysts of specific reactions such as the Hydrogen Evolution Reaction (HER) and the Oxygen Evolution Reaction (OER) (Mahmood et al., 2018). Polarization plot generated by LSV is a plot of the response current versus the potential swept. These LSV plots give us important performance metrics. These are the amount of overpotential required to achieve a specific benchmark current density (a common benchmark for HER/OER is 10 mA cm^{-2}) and the amount of current density that may be maintained at a specific applied overpotential by the catalyst. Lower overpotential

required attaining a desired current density, or higher current density achieved at a specific overpotential, demonstrates better catalytic activity.

Tafel analysis is based on the tafel equation, $\eta = a + b \log j$, showing a relationship between overpotential (η) and log of the current density (j). A tafel plot can thus be prepared by plot of overpotential usually along the y-axis vs. log of the current density along the x-axis (van der Heijden et al., 2024). Here in this linear part of the plot, the slope is the tafel slope (b), and intercept (ideally at zero overpotential) gives the exchange current density (j_o). The tafel slope (b) is an intrinsic kinetic parameter that conveys information on the Rate Determining Step (RDS) and overall reaction pathway of an electrochemical reaction. Different theoretical tafel slopes relate to specific RDSs: roughly < 30 mV/dec for the tafel step, 40-120 mV/dec for the heyrovsky step, and >120 mV/dec for the volmer step. Comparison of the experimentally observed tafel slope with these theoretical values helps the researcher draw an inference of the operating mechanism. The exchange current density (j_o), as obtained from the intercept of the tafel plot, is the built-in catalytic activity of the electrode material at the equilibrium potential. Higher j_o implies kinetics near equilibrium happen faster.

3.3.2.2 Cyclic Voltammetry (CV)

Cyclic voltammetry (CV) is a highly versatile electrochemical technique in which the potential of the working electrode is swept linearly between two predefined limits (an initial potential and a final potential) at a constant rate (Elgrishi et al., 2018). The direction of the potential sweep is then reversed, and the potential is swept back to the initial value. The present response of the electrochemical cell is monitored constantly as a function of applied potential, generating a graph called a cyclic voltammogram (CV curve). CV experiments yield useful data on redox potentials of species in the system, reversibility of electron transfer reactions, and capacitive currents at the electrode-electrolyte interface. This technique is generally carried out using a standard three-electrode cell setup, which consists of a working electrode, a reference electrode, and a counter electrode. Within electrocatalysis, CV is utilized in a number of significant manners. Cyclic potential sweeps are often used to electrochemically activate or condition the surface of a catalyst prior to making initial activity measurements, for example Linear Sweep Voltammetry (LSV) (Elgrishi et al., 2018).

Activation can desorb surface impurities, cause restructuring of the catalyst surface, or enable in situ creation of the actual catalytically active phase under electrochemical conditions. The shape and specific features observed in CV curves can also provide qualitative information regarding the electrocatalytic activity of the catalyst and the incidence of connected redox processes.

3.3.2.3 Electrochemical impedance spectroscopy (EIS)

Electrochemical impedance spectroscopy (EIS) is one of the AC techniques used to study the impedance behavior of an electrochemical system. It involves superimposition of a small amplitude sinusoidal voltage or current disturbance on the working electrode over a wide range of frequencies and measurement of the resulting sinusoidal current or voltage response (Lazanas & Prodromidis, 2023). The impedance (Z) is a complex variable with real (resistance, Z') and imaginary (reactance, Z") components, and these components are a function of the frequency of the applied perturbation. The EIS data is typically plotted in the form of Nyquist plots (a plot of -ImZ vs. ReZ) or Bode plots (a plot of the logarithm of the impedance magnitude and the phase angle vs. the logarithm of the frequency). EIS is so effective technique because it can separate various physical and electrochemical processes occurring in the system that occur in various timescales (frequencies), e.g., charge transfer kinetics, mass transport phenomena, and capacitive effects at the interface (Magar et al., 2021). It is being utilized heavily to assess charge transfer kinetics. The charge transfer resistance (R_{ct}), which is typically represented by a semicircle in the Nyquist plot and is derived from fitting the data, is inversely proportional to the rate of electron transfer at the electrode-electrolyte interface. Lower the R_{ct} value, the faster the charge transfer kinetics and, hence, the greater the catalytic activity. EIS is commonly utilized for making comparisons among the R_{ct} values of different electrocatalyst materials.

3.3.2.3 Chronoamperometry (CA) and Chronopotentiometry (CP)

Chronoamperometry (CA) and Chronopotentiometry (CP) are time-domain electrochemical techniques used to study the response of an electrochemical system to specified conditions. In CA, the working electrode is applied at a specified potential, and the resulting current is monitored as a function of time. In CP, the working electrode is applied at a specified current, and the resulting potential is monitored as a function of time (Rafiee et al., 2024). Both techniques provide information about

reaction kinetics and mass transport under these constant electrochemical conditions. CA and CP tend to be employed to assess long-term operational stability of electrocatalysts under conditions that are pertinent to their own practical applications (Zhai et al., 2022). In CA, catalyst stability is checked by monitoring the current response with time under a constant applied potential; a stable catalyst is one where the current is relatively stable with minimal decay. In CP, stability is checked by monitoring the potential response with time under a constant applied current density; a stable catalyst experiences minimal rise in potential. Such stability tests may be performed for extended periods, from a few hours to days or even weeks, to mimic realistic operating times. The test parameters, i.e., the potential or current density applied, time, and the electrolyte composition, are selected to be suitable for the anticipated application. Chronoamperometry and chronopotentiometry provide the simplest assessment of catalyst performance under steady-state conditions over extended periods and therefore mimic practical use conditions. Although techniques like CV cycling are useful in accelerating degradation and durability testing, chrono techniques mimic steady-state operation at constant potential or current. The observation of present response over time in CA or the potential response over time in CP clearly points to how well the catalyst maintains activity under sustained burden. It is a significant test for practical application, as a catalyst can exhibit high initial activity and good performance during accelerated CV testing but deteriorate under prolonged steady-state operation from reduced rates of degradative processes unseen in aggressive cycling.

3.3.3 Electrochemical set up

All electrochemical measurements were performed in a conventional three-electrode cell using a BioLogic SP300 Potentiostat electrochemical workstation. A working electrode was made using a method outlined previously (Ha et al., 2023). The counter electrode consisted of a platinum wire, and a Ag/AgCl electrode served as the reference electrode.

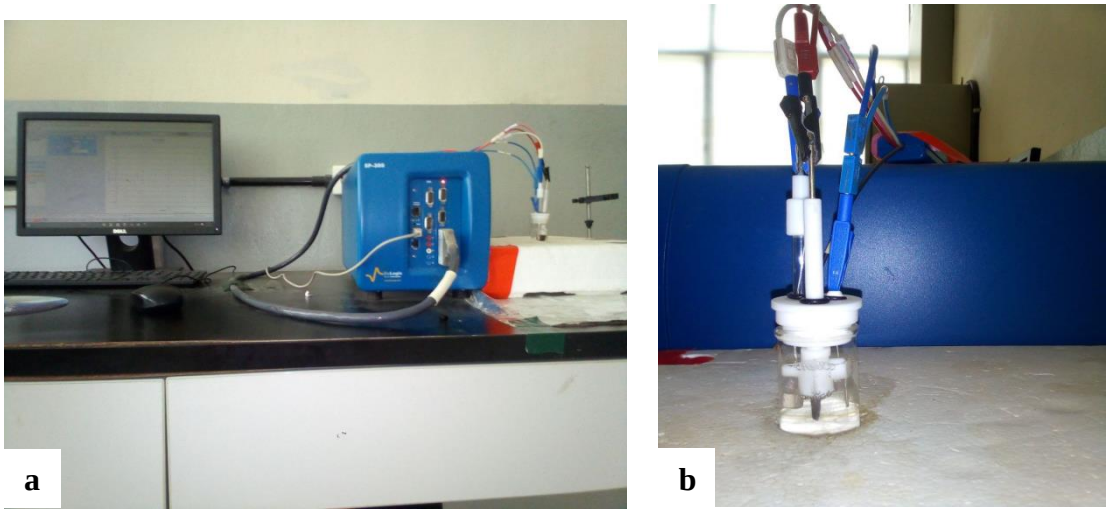

Figure 3. 3: (a) Electrochemical characterization set up (b) Three electrode system

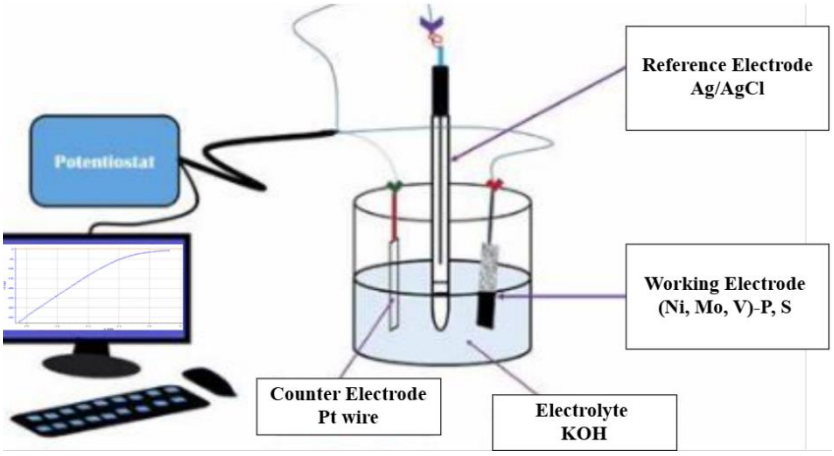

Figure 3. 4: Schematic representation of electrochemical characterization set up

All potentials in the paper are given with respect to the reversible hydrogen electrode (RHE) and calculated using Equation 3.1, where E (RHE) potential relative to the RHE, E (Ag/AgCl) is measured potential relative the Ag/AgCl electrode, pH is the pH of electrolyte, and E_o (Ag/AgCl) is the standard potential of the Ag/AgCl electrode at 25^{o}C, which is 0.1976 V. The data was collected without iR compensation. The voltages were recalculated to the RHE potential according to the Nernst equation, and the preliminary pH values of the solutions utilized in the experiments were measured.

$$E_{RHE} = E_{Ag/AgCl} + 0.059\ pH + E_{oAg/AgCl} \quad (3.1)$$

Because of the concern that there are problems which arise from incomplete wetting, the first step was to keep the working electrode submerged within the electrolyte for

30 min. The OCP was measured for a time period of 60 seconds to ensure that there was valid connection in the circuit and for the fluctuation in the OCP indicating the complete wetting. To determine the activity and extract other important information, LSV and CV conducted at smallest scan rate. The value of overpotential was calculated by using Equation 3.2 where η is overpotential, and E_o is the thermodynamic potential to evolve hydrogen.

$$\eta = E_{RHE} - E_o \quad (3.2)$$

The LSV were used to create Tafel plots, which display overpotential versus log (current density), and the linear region at low overpotential was fit to the Tafel equation using Equation 3.3

$$\eta = b\log j + a \quad (3.3)$$

Where j is current density, b is Tafel slope and a is constant

To reliably measure the activities and other information obtained, the electrochemical activation of the catalyst-and-the inferences was stabilized by conducting rapid cycling using CV at relatively high scan rates ($100mVs^{-1}$) during an initial period of 50 cycles, where the change in the overpotential at fixed current density must be monitored with respect to the cycle number. The LSV and CV were conducted at the smallest scan rate again to show that the catalyst is stable even after such harsh high-scan-rate CV cycling and that the results obtained previously are reliable. EIS at catalytic turnover conditions was conducted to elaborate on the origin of the activity and drawing comparisons with other electrodes, which was screened consecutively. The EIS data were fitted with the electrochemical workstation inbuilt Z-fit EIS analysis software.

Finally, constant voltage was carried out to show that the catalyst of choice is keeping excellent stability under such operation conditions which could enable it to benchmark.

CHAPTER FOUR
RESULT AND DISCUSSION

4.1 Introduction

To evaluate the structural features and electrocatalytic performance of the synthesized material, a wide variety of characterization techniques was employed. Structural, morphological, elemental, and surface chemistry examinations were performed together with electrochemical tests to comprehend the catalytic behavior in greater detail. The elemental and compositional analyses confirmed the successful synthesis of multi-element-doped Ni-based electrocatalysts. X-ray diffraction (XRD) was employed to investigate the crystalline structure and phase composition of the synthesized (Ni, Mo, V)-P, S electrocatalysts. This technique is essential for confirming the formation of target compounds and detecting any structural changes resulting from elemental doping. Scanning electron microscopy (SEM) revealed the porous and roughened surface morphology of the (Ni, Mo, V)-P, S sample suitable for HER. Energy-dispersive X-ray spectroscopy (EDS) confirmed the uniform distribution of the Ni, Mo, V, S, and P elements on the surface of the catalyst, confirming efficient multi-element incorporation. X-ray photoelectron spectroscopy (XPS) further disclosed the existence of different species, which are believed to play a synergistic role in enhancing the catalytic activity. Electrochemical tests demonstrated the excellent HER activity of the (Ni, Mo, V)-P, S catalyst with a low overpotential of -53 mV at 10 $mAcm^{-2}$ and long-term stability for 30,000 seconds at 100 $mAcm^{-2}$. Electrochemical impedance spectroscopy (EIS) showed the lowest charge transfer resistance (Rct) of 1.2 Ω among all samples, indicating fast electron transfer kinetics. All these findings suggest that the combination of uniform elemental distribution, and benign electronic interaction synergistically enhances the electrocatalytic activity and stability of the (Ni, Mo, V)-P, S catalyst.

4.2 Structural Characterization

X-ray diffraction (XRD) was employed to confirm the crystal structures of the electrochemically deposited electrocatalysts. Given the complexity and possible amorphous nature of the materials, XRD phase identification relies on the most

prominent peaks, as weaker signals from dilute or disordered phases may be undetectable. The XRD patterns of the synthesized NiMoV, (Ni, Mo, V)-P, and (Ni, Mo, V)-P, S heterostructure are presented in Fig. 4.1. The XRD patterns of all samples exhibit diffraction peaks at $2\theta \approx 43.5°$ and 75.58°, corresponding to the (200) and (300) planes of NiO (JCPDS No. 03-065-2901) and a separate peak at $2\theta \approx 51.0°$ was observed and is attributed to the (200) plane of metallic Ni (JCPDS No. 04-0850). The presence of both phases suggests that Ni exists in a mixed metallic and oxidized state on the surface, possibly due to air exposure during post-synthesis (Salunkhe et al., 2020). The appearance of those peaks revealed that the resultant particles were pure face centred cubic (fcc) nickel. The strong and narrow diffraction peaks indicated that the product had a well-crystalline structure, indicating the crystalline nature of the Ni support (Jayaseelan et al., 2014). The characteristic peaks of (Ni, Mo, V)-P at 30.4° correspond to metallic P. The prominent peak of diffraction is attributed to (222) planes of a cubic crystal structure, suggesting that the obtained phosphorus matches well with JCPDS No. 41-1105 (Rafiaei, 2018). The (222) peak appears at 23.3°**.** The presence of the (222) peak in (Ni, Mo, V)-P , S is consistent with elemental sulfur (S_8)**,** often seen in nanoparticle form (Suleiman et al., 2015). The presence of VO_2 was confirmed by the appearance of characteristic diffraction peaks at approximately 13.1°, corresponding to the (110) plane, which matches well with the JCPDS card #65-7960 (Bouzbib et al., 2023). Notably No distinct diffraction peaks corresponding to molybdenum or Phosphorus were observed. This may be due to the low concentration, high dispersion, or amorphous nature of these phases. It is also possible that Mo and P are incorporated into the Ni-based lattice, forming solid solutions or highly disordered phases that are undetectable by conventional XRD. However, as illustrated in Fig. 4.1 (a), the (Ni, Mo, V)-P and (Ni, Mo, V)-P, S sample exhibited a marked reduction in peak intensity and increased baseline noise, which could be attributed to lower crystallinity or partial amorphization induced by phosphorus and sulfur doping. This structural disorder may contribute to enhanced electrocatalytic activity by increasing the number of exposed active sites and defect density.

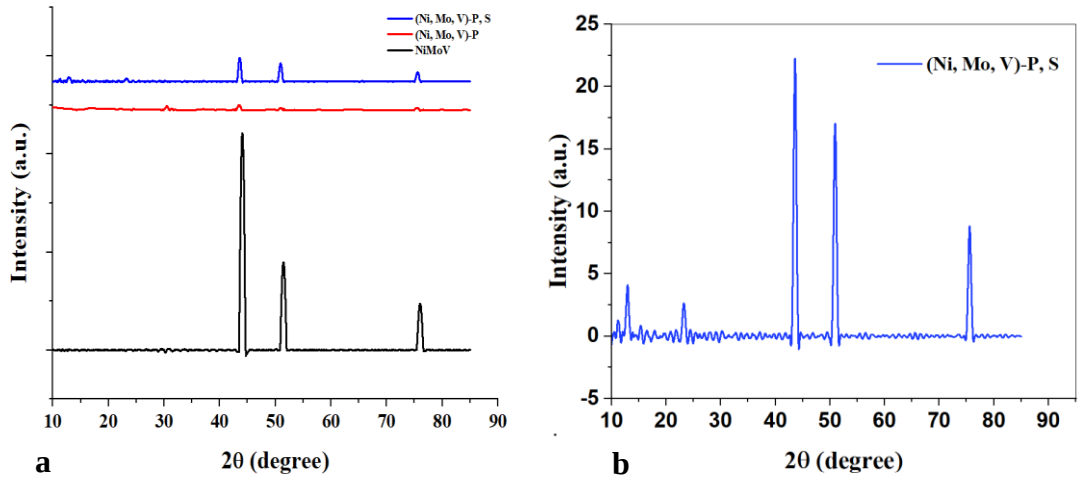

Figure 4. 1: (a) XRD patterns (b) magnified XRD of (Ni, Mo, V)-P, S

4.3 Morphology analysis

SEM offers a high resolution imaging that is vital for understanding complex morphological features in materials across an array of length scales. Figure 4.1 (a) reveal the overall macrostructure of the sample, presenting evidence of a highly porous, 3D interconnected network, which is a characteristic common to foam or mesh substrate such as Ni foam (Chaudhari et al., 2017). The struts that constitute the skeleton and the large pores are observable. A coating material is observed on the struts of the substrate in all SEM images. This coating gives the struts a rougher, slightly granular texture. The coating appears to provide a uniform cover to the visible surfaces of the substrate skeleton throughout the magnification range. There are no apparent large-scale patchy areas or areas where the substrate seems uncoated, indicating complete coverage and uniform coating by hydrothermal synthesis. The SEM image in Figure 4.1 (b) gives a closer view of the coating on the foam struts. The coating is clearly resolved to be composed of grouped smaller particles or structures, providing rough and textured surface. Figure 4.1(c) indicates morphology with highly aggregated particles. Instead of discrete, individual units, the material is composed of large, irregular clusters. Figure 4.1(d)-(f) clearly reveals that the surface of the larger micrometer-scale agglomerates is densely covered by smaller, well-defined structures. These structures strongly resemble nanosheets, rather than distinct nanowires or nanorods. These nanosheets are highly interconnected and appear to grow outwards, creating a complex, hierarchical structure. Nanosheets and particularly their fine edges are key HER active sites (Ni & Wang, 2015). The process

of synthesis produced particle/clusters formation and aggregation rather than a conformal, smooth film. The surface looks quite rough, with densely packed. There is also no evidence of large cracks within the coating layer, delamination from the substrate, or large areas of bare substrate from low to high magnification of the coating layer. The SEM images indicate that the hydrothermal synthesis method did promote this complete and widespread coverage over a complicated, high-surface-area, three-dimensional structure of the foam substrate. Instead of producing a smooth, conformal layer, the hydrothermal synthesis caused particles or clusters to form and aggregate.

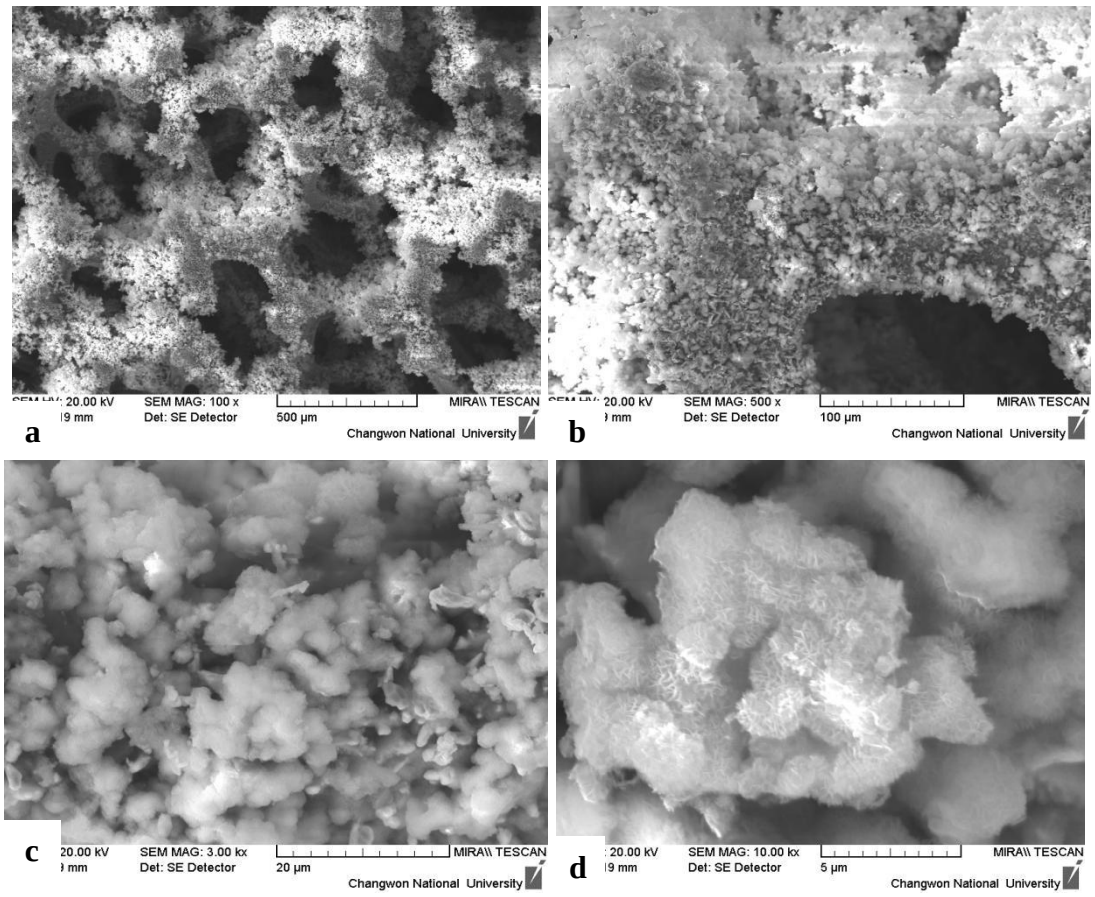

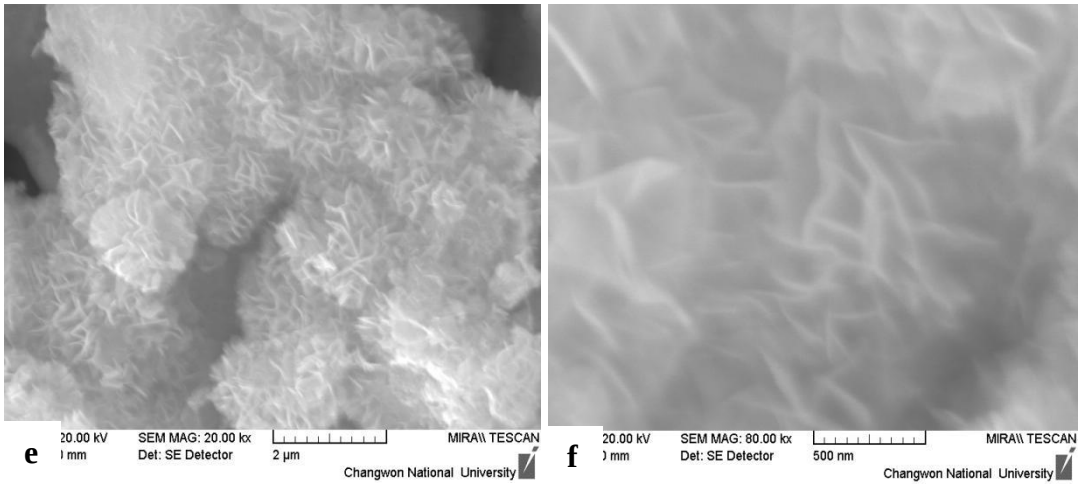

Figure 4. 2: SEM image (a) 100 x (b) 500 x (c) 3.00 kx (d) 10.00 kx (e) 20.00 kx(f) 80.00 kx

Energy-dispersive X-ray spectroscopy (EDS) serves primarily to verify that all elements intended during synthesis are successfully incorporated into the resulting material (Hodoroaba, 2020). According to the maps, it is revealed that the analyzed area (Area 10) contains Oxygen, Phosphorus, Molybdenum, Sulphur, Vanadium, and Nickel. The EDS elemental mapping reveals varying spatial distributions for each element on the electrocatalyst surface. Oxygen (O K map) is observed to be uniform and is more strongly associated with the larger agglomerate areas. Phosphorus (P K map) reveals a relatively diffuse distribution, indicating its extensive incorporation in the catalyst matrix. Molybdenum (Mo L map) is strongly enriched in the finer morphology. Sulfur (S K map) mirrors this profile closely. Vanadium (V K map), by contrast, is selectively enriched in the larger agglomerate domains. Nickel (Ni K map) presents a diffusely spread appearance across both finer and agglomerated zones with a very slightly elevated intensity in the agglomerated regions or on coatings on the surface, which suggests its role as a structural or conductive framework across the catalyst.

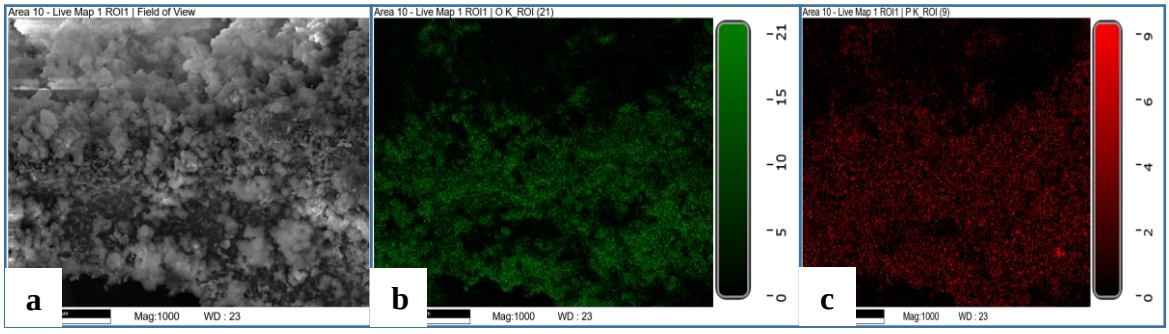

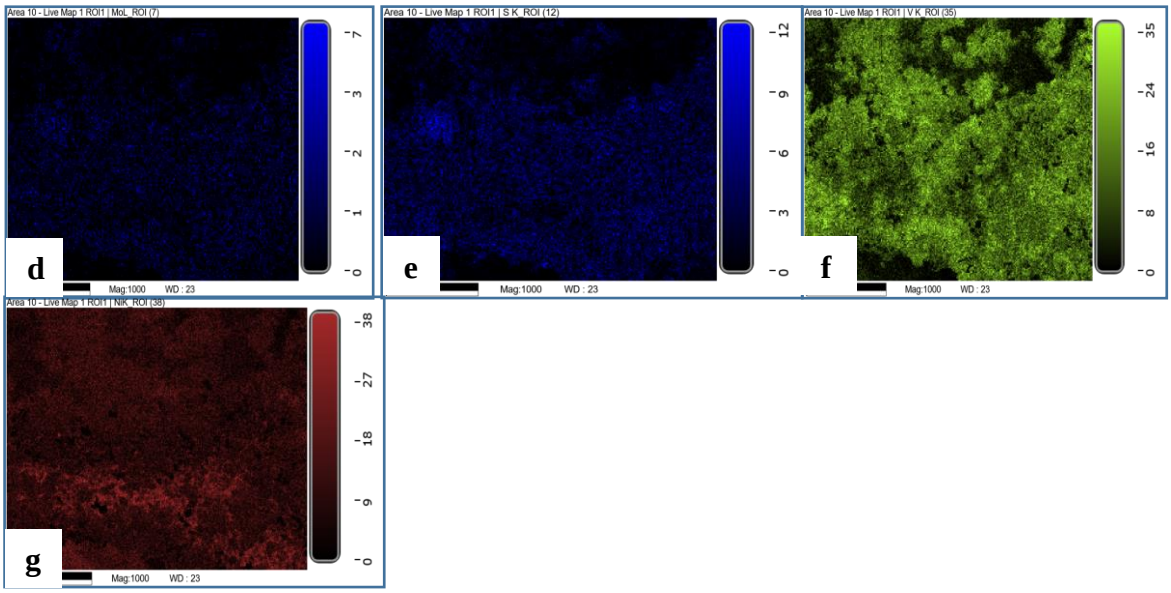

Figure 4. 3: (a) SEM , EDS for (b) Oxygen (c) Phosphorus (d) Molybdenum (e) Sulfur (f) Vanadium (g) Nickel

Quantitative results from the Energy Dispersive X-ray Spectroscopy (EDS) show that the major constituents of the material were nickel (Ni) at 55.7 weight percent (40.1 atomic percent), vanadium (V) at 30.4 weight percent (25.2 atomic percent), and oxygen (O) at 12.6 weight percent (33.1 atomic percent). The large proportion of oxygen, particularly the high atomic percentage, strongly implies that these metals are in their oxide forms. The analysis also indicated the presence of very small quantities of phosphorus (P) at 0.2 weight percent (0.3 atomic percent) and molybdenum (Mo) at 0.2 weight percent (0.1 atomic percent), and another trace amount of sulfur (S) at 1.0 weight percent (1.3 atomic percent).

Table 4. 1: EDS quantitative results

Element	Weight %	MDL	Atomic %
O K	12.6	0.28	33.1
P K	0.2	0.04	0.3
S K	1.0	0.04	1.3
V K	30.4	0.07	25.2
Ni K	55.7	0.14	40.1
Mo L	0.2	0.11	0.1

4.4 Surface Elemental Composition and Chemical State Analysis

The X-ray Photoelectron Spectroscopy (XPS) data of the catalysts gives insights for surface elemental composition and chemical state of the electrocatalyst. High points in the data are identified and related to known binding energies. The Mo 3d data in Figure 4.2 (a) spans approximately from 222 eV to 242 eV. Significant intensities are noted around 232-233 eV and 235-236 eV. The peaks at 232.35 eV can be attributed to Mo $3d_{5/2}$ and 235.46 eV peak to Mo $3d_{3/2}$. These binding energies are normal for Molybdenum in relatively high oxidiation states as the Mo^{4+}, e.g. or MoS_2 or MoO_2 or Mo^{6+}, e.g for in MoO_3. The binding energy at 232-233 and 235-236 corresponds to MoS_2 and MoO_3, respectively (NIST X-ray Photoelectron Spectroscopy Database (SRD 20), Version 5.0, 2023).

The energy interval of the Ni 2p data as shown in Figure 4.2 (b) is about 840 eV to 890 eV. The high intensities are found at 853–856 eV and at 870–874 eV, further strong intensities are observed at 860–862 eV and 879–881 eV. The Ni 2p spectrum is complicated with contributions from the spin orbit doublet (Ni $2p_{3/2}$ and Ni $2p_{1/2}$) and satellite peaks. Peaks at 855 eV for the Ni $2p_{3/2}$ and 872.5 eV for the Ni $2p_{1/2}$ would be indicative of Ni^{2+} or Ni^{3+} states (Guzman-Bucio et al., 2023). The features of NiO species are observed around 854-856 eV in Ni $2p_{3/2}$.The other enhanced intensities at 860.5 eV and 878.4eV are satellite peaks of Ni^{2+} speciation (NIST X-ray Photoelectron Spectroscopy Database (SRD 20), Version 5.0, 2023). The range of the O 1s data as shown in Figure 4.4 (c) is ~525 eV-545 eV. The peak near 529.65 eV is associated frequently with metal-oxygen bonds (M-O) in oxides (i.e., NiO) (Velázquez-Hernández et al., 2023) (NIST X-ray Photoelectron Spectroscopy Database (SRD 20), Version 5.0, 2023). Features at slightly higher binding energies (approximately 531.19 eV) can be attributed to V_2O_3, $VOPO_4$, V_2O_5 or to oxygen in either the defect sites or oxygen vacancies, which may be beneficial for HER (Wang et al., 2024) (NIST X-ray Photoelectron Spectroscopy Database (SRD 20), Version 5.0, 2023).

The S2p data in Figure 4.4 (d) extends from about 155 eV up to 175 eV. High intensities are seen at ~162 eV with some intensity also seen between 169.66 eV. The presences of peaks in the region of 162 eV for the S $2p_{3/2}$ level are typical for

metal-sulfides (M-S) (NIST X-ray Photoelectron Spectroscopy Database (SRD 20), Version 5.0, 2023). For instance in MoS_2 is found at about 162-163 eV (Chanturiya et al., 2019). Peaks at 169.66 eV can also correspond to sulfates (Ha et al., 2023). The V2p set of data in Figure 4.4 (e) ranges from 508 eV to 525 eV. The $V2p_{3/2}$ peak is visible around 516 eV. This binding energy fits for Vanadium in several oxidation states, for example V^{4+} or V^{5+} in oxides as VO_2 (V^{4+} 515.7-516.5 eV) (Silversmit et al., 2004). The appearance of oxygen indicates that vanadium possibly presents as vanadium oxides (VO_x) such as V_2O_3 (NIST X-ray Photoelectron Spectroscopy Database (SRD 20), Version 5.0, 2023). In conclusion, XPS results indicate that a complex multicomponent material was formed on the nickel foam. Some of the key ingredients are sulphides and/or oxides of molybdenum, Nickel oxides and Vanadium oxides (NIST X-ray Photoelectron Spectroscopy Database (SRD 20), Version 5.0, 2023).

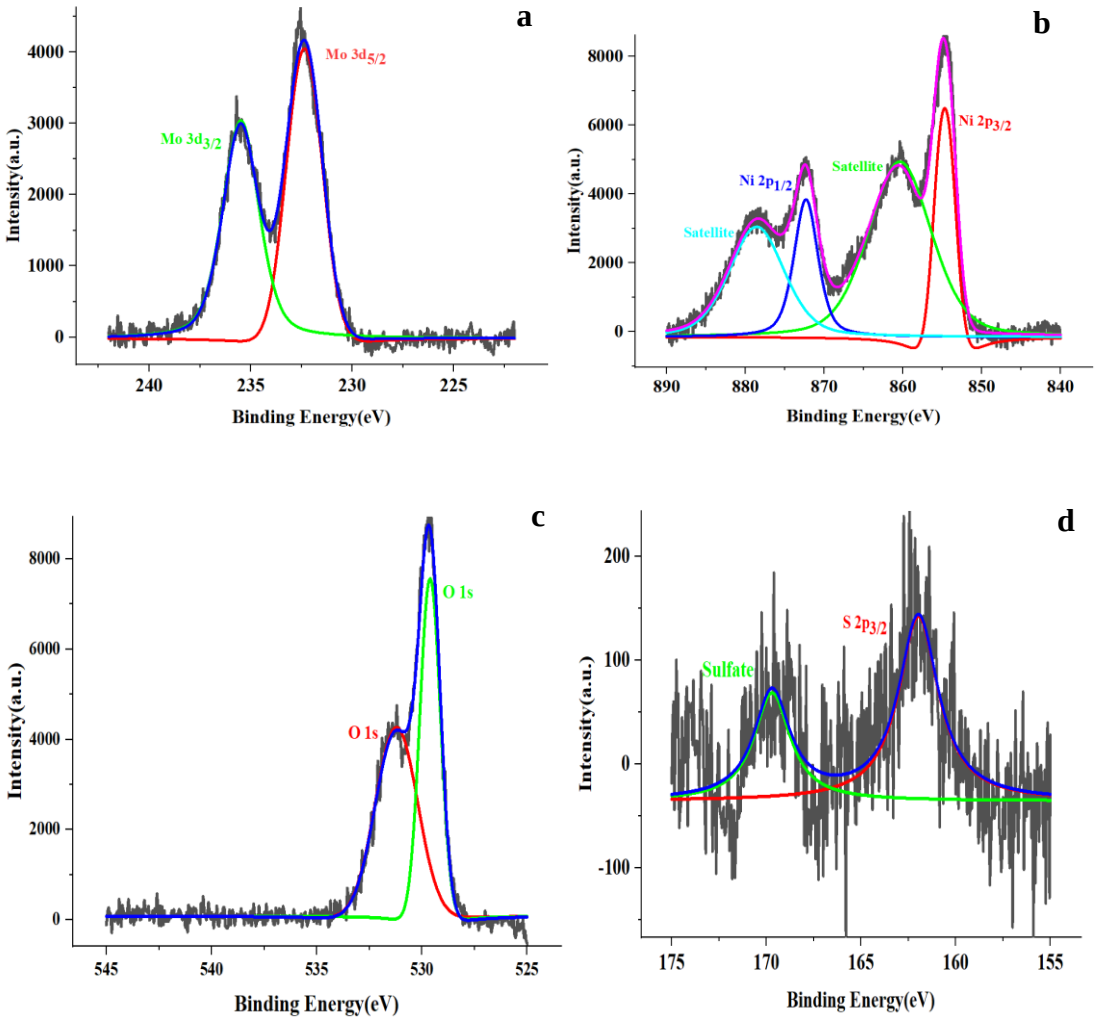

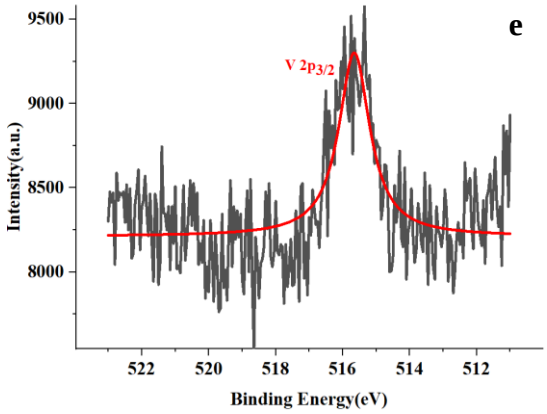

Figure 4. 4: XPS (a) Mo 3d (b) Ni 2p (c) O 1s (d) (e) S 2p (f) V 2p

4.5 Electrochemical analysis

4.5.1 Effect of Phosphorus Doping on HER Electrocatalytic Performance

Phosphorus doping has a significant effect on the modulation of the electrochemical performance of NiMoVP electrocatalysts toward the hydrogen evolution reaction (HER) in an alkaline medium. To delve into the effect of phosphorus incorporation, the concentration of phosphorus precursor was varied at 0.01, 0.05, 0.1, and 0.15 mmol, which was assigned NiMoVP-0.01, NiMoVP-0.05, NiMoVP-0.1, and NiMoVP-0.15, respectively. Their activities toward HER were compared in terms of the overpotential required to reach a fixed current density of 10 $mAcm^{-2}$ and the maximum current density achieved via linear sweep voltammetry.

Table 4. 2: Effect of Phosphorus Doping Concentration on the HER Performance of NiMoVP-x Electrocatalysts

Sample	P (mmol)	Overpotential @10 mA/cm² (mV)	Max Current Density (mA/cm²)
NiMoVP-0.01	0.01	-135	182
NiMoVP-0.05	0.05	-100	202
NiMoVP-0.1	**0.1**	**-80**	**260**
NiMoVP-0.15	0.15	-90	221

The variation in HER activity with phosphorus doping shows a non-linear trend, reflecting its complex effect on the catalytic behavior of NiMoV-based materials. The overpotential significantly decreases from 135 mV to 100 mV as the phosphorus content rises from 0.01 to 0.05 mmol, while the current density slightly increases from 182 to 202 mA/cm². This improvement can be attributed to phosphorus-induced modulation of the electronic environment, which likely enhances charge redistribution around the metal centers (Ni, Mo, V), facilitating better charge-transfer kinetics. Phosphorus, acting as an electron-withdrawing element, may also promote exposure of catalytically active sites by introducing favorable surface strain or altering local coordination structures. HER activity is further improved by raising the phosphorus concentration to 0.1 mmol, with the overpoten1tial dropping to 80 mV and the current density increasing to 260 mA/cm^2. However, this enhancement becomes more gradual, indicating that the system is approaching a saturation point where the benefits of phosphorus doping begin to plateau. Beyond this point, excessive incorporation may lead to negative effects that offset the earlier gains.

Further increasing the phosphorus concentration to 0.15 mmol begin to saturate the catalyst's surface, blocking or passivating active sites critical for hydrogen adsorption and desorption yields an overpotential of 90 mV and a maximum current density of 221 mA/cm^2. This surface site coverage can reduce the availability of exposed metal centers, thereby diminishing the intrinsic catalytic efficiency even if geometric current density appears high. Moreover, excess phosphorus may disrupt the optimal local coordination of the metal sites, potentially inducing lattice distortions, electronic disorder, or formation of inactive phosphate-like surface phases. These effects can compromise the structural integrity and long-term stability of the catalyst. Excess phosphorus may adversely affect the electronic structure to inhibit H^+ ions adsorption or to reduce kinetically H–H bond formation, causing degradation of catalytic selectivity and efficiency. Potential deactivation mechanisms further emphasis the utmost necessity in optimizing phosphorus content toward maximization of HER activity and prevention of degrading effects that embarrass over doping.

While moderate phosphorus incorporation improves HER performance through enhancement of electron distribution and exposure of catalytic sites, over-doping may bring about detrimental performance consequences. NiMoVP-0.1 endorses the best balance, which means that utmost dopant tuning is required for greatest activity.

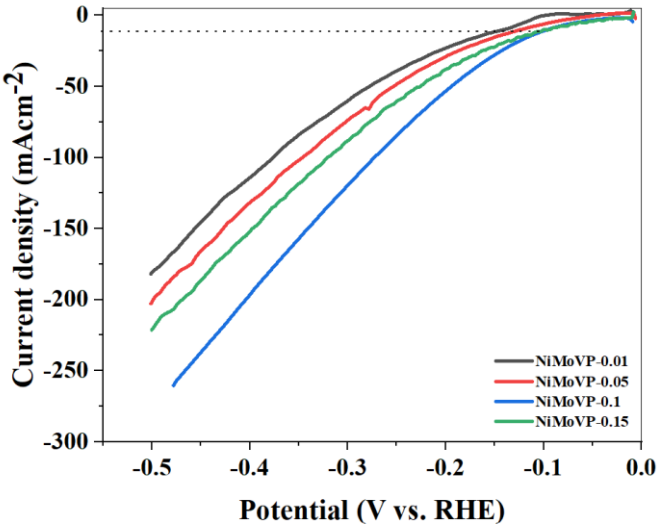

Figure 4. 5: LSV on effect of phosphorus doping on HER performance

4.5.2 Effect of Sulfur Doping on HER Electrocatalytic Performance

Sulfur doping also plays a significant role in the chemical activity tuning of the NiMoVPS series for the hydrogen evolution reaction (HER) in alkaline media. The sulfur content was varied from 0.1 to 0.25 mmol, so the corresponding samples are NiMoVPS-0.1, NiMoVPS-0.15, NiMoVPS-0.2, and NiMoVPS-0.25. The HER performances are evaluated in terms of overpotential at 10 mA cm^{-2} and maximum current density obtained during linear sweep voltammetry.

Table 4. 3: Effect of Sulfur Doping Concentration on the HER Performance of NiMoVPS-x Electrocatalysts

Sample	S (mmol)	Overpotential @10 mA/cm² (mV)	Max Current Density (mA/cm²)
NiMoVPS-0.1	0.1	-86	182
NiMoVPS-0.15	0.15	-73	247
NiMoVPS-0.25	0.25	-71	360
NiMoVPS-0.2	**0.2**	**-53**	**372**

The observed nonlinear relationship between sulfur doping concentration and HER performance suggests complex underlying mechanisms affecting the catalytic activity of (Ni, Mo, V)-P, S electrocatalyst. Improved catalytic kinetics are implied by the overpotential dropping sharply from 86 to 53 mV and the current density rising sharply from 182 to 372 mA/cm² as the sulfur content rises from 0.1 to 0.2 mmol.

This enhancement is probably due to changes in the electronic structure brought about by sulfur, such as a higher electron density at active metal centers (Ni, Mo, and V), which promote quicker charge transfer and better hydrogen adsorption/desorption behavior. Furthermore, heteroatom-induced strain or surface defects may be introduced by proper sulfur doping and serve as extra active sites.

When the sulfur concentration is raised to 0.25 mmol, even though the current density stays relatively high at 360mA/cm2, a slight increase in overpotential to 71 mV is seen. This variation raises the possibility that too much sulfur could affect the catalyst in two ways. Oversaturation of active sites, where too many sulfur atoms occupy or block catalytically relevant surface positions, is one conceivable mechanism that prevents hydrogen from adsorbing or desorbing. The ideal coordination environment needed for HER may also be disrupted by high sulfur loading, which can also cause surface restructuring, increased disorder, or the formation of inactive sulfur-rich phases. Despite an apparent increase in geometric current density, such structural perturbations can lower the catalyst's intrinsic activity.

Moderate doping helps HER activity by influencing surface electronic character and by creating a high density of catalytic sites; over doping breaks this balance and introduces a pathway toward deactivation. It is therefore of paramount importance for dopant engineering not only to realize optimal performance but also to sustain long-term structural integrity and catalytic efficiency.

Thus, NiMoVPS-0.2 exhibited the best electrocatalytic behaviour with a lower overpotential and highest current density, which illustrates this as the optimal concentration of sulfur doping necessary for efficient HER. It becomes evident from the results that careful adjustment of the dopant levels is necessary to achieve a balance between the structural and electronic effects for designing high-performance electrocatalysts.

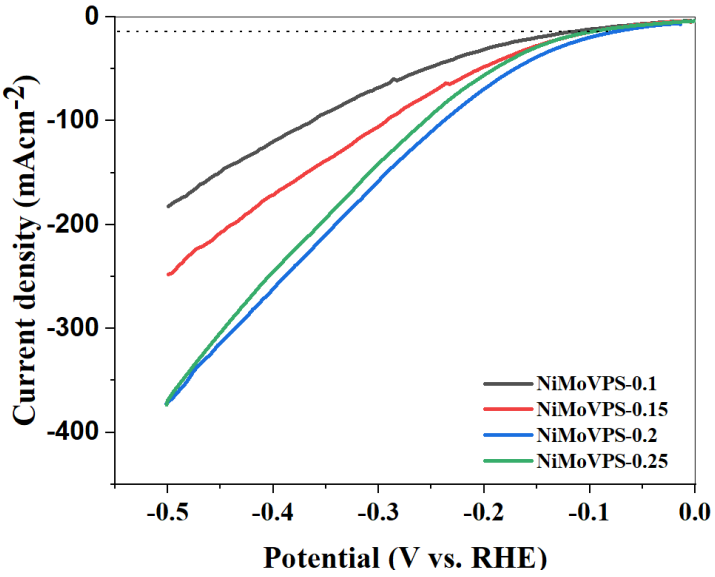

Figure 4. 6: LSV on effect of sulfur doping on HER performance

4.5.3 Electrolytic performance of (Ni, Mo, V)-P, S and controlled samples

4.5.3.1 LSV

The water splitting reaction requires a voltage greater than 1.23 V. The extra voltage beyond the thermodynamical limit is termed overpotential, η. The extra energy required arises mainly due to the limitations arising from the mass transfer and ohmic losses across the electrolyte (Raveendran et al., 2023). The LSV data presented in Figure 4.4 (a) make it clear that the multi-component (Ni, Mo, V)-P, S catalyst is the most promising material for HER among those tested, primarily due to its higher current density of 350mA and considerably lower overpotential, -0.053 V Vs RHE @10mAcm^{-2}. Through the other materials, this catalytic composition is claimed to be the most active for HER. For example, In NiMo, at a current density of 10 mA cm^{-2}, an overpotential of around -0.154 V is required, whereas in NiMoV the value is -0.135 V, and in (Ni, Mo, V)-P -0.080 V. Thus, the trend clearly shows that HER is enhanced by the further addition of elements such as V, S, and P to the base NiMo catalyst. (Ni, Mo, V)-P, S exhibits the highest current density at any applied potential Synergistic effects between Ni, Mo, V, S, and P can be presumed from the gradual improvement. It would seem that every constituent enhances electrical conductivity, increases active site numbers, or improves hydrogen adsorption/desorption kinetics and intrinsic catalytic activity. The (Ni, Mo, V)-P, S catalyst gives the smallest overpotential at particular current densities. That is to say, it attains appreciable current densities (e.g., > 350 mAcm^{-2}) at a potential where all others are substantially

lesser active. The very thing found to be key to energy-efficient hydrogen production is the lower overpotential. In sum, the extraordinary activity observed is attributed directly to the synergistic combination of phosphorus, sulfur, and vanadium additions to the nickel molybdenum system. The enhanced HER activity of the (Ni, Mo, V)-P, S electrocatalyst, distinguished by its superior current density and much lower overpotential in the LSV curves, is directly related to surface chemistry as revealed by XPS. Surely, (Ni, Mo, V)-P, S is promoting the formation of a higher concentration of active sites or better active sites, as evidenced by XPS analyses (Mo3d, Ni2p, O1s, S2p, and V2p). The synergistic effect of all these components may change the electronic structure and surface morphology in a way that promotes proton adsorption, electron transfer, and hydrogen desorption, all needed for efficient HER.

In Figure 4.4(b), The overpotential of various catalysts towards the hydrogen evolution reaction (HER) shows a definite trend in activity, with commercial Pt/C (not tested herein but used as a reference benchmark) exhibits lowest overpotential values widely reported at approximately -36 mV at 10 mA cm^{-2}. In this work, (Ni, Mo, V)-P, S displays the optimum HER performance among the fabricated catalysts with overpotentials of -53, -174, and -242 mV at 10, 50, and 100 mA cm^{-2}, respectively, due to synergistic effects caused by multi-element doping and sulfur incorporation facilitating charge transfer and active site exposure. The (Ni, Mo, V)-P catalyst subsequent to overpotentials slightly higher of -81, -191, and -272 mV indicates the role of phosphorus alone towards greater activity. The (Ni, Mo, V) system without both P and S has even higher overpotentials of -138, -235, and -310 mV, indicating reduced conductivity and lower active sites. Lastly, the (Ni, Mo) catalyst has the worst performance with the highest overpotentials over -445 mV at 100 mA cm^{-2}, which reflects on the effectiveness of vanadium and dopant tuning in enhancing HER activity.

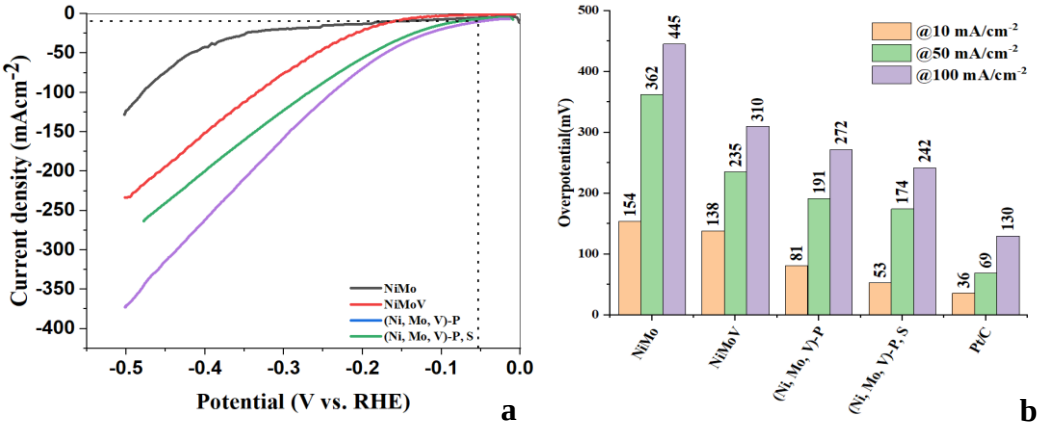

Figure 4. 7: (a) LSV (b) Overpotential

4.5.3.2 EIS

Data from electrochemical impedance spectroscopy (EIS) is used to create a Nyquist plot (Lazanas & Prodromidis, 2023). The plot displays, in ohms (Ω), the real part of the impedance (Re (Z)) on the x-axis and the imaginary part (−Im(Z)) on the y-axis for the four distinct materials. The charge transfer resistance (R_{ct}), a measurement of the resistance to electron transfer during the electrochemical reaction, is correlated with the diameter of each semicircle (Lou & Chen, 2015). The most effective charge transfer at the electrode-electrolyte interface is indicated by (Ni, Mo, V)-P, S 1.2 Ω smallest R_{ct}. This implies that (Ni, Mo, V)-P, S is the best electrocatalyst among the materials tested, most likely as a result of improved conductivity or active sites brought by sulfur and phosphorus doping. The highest resistance to charge transfer, as indicated by NiMo, can be associated with lower electrocatalytic activity and mass transport limitations. The trend (NiMo (42.03 Ω) > NiMoV (22.08 Ω) > (Ni, Mo, V)-P (3.6 Ω) > (Ni, Mo, V)-P, S (1.2 Ω)) indicates that adding phosphorus (P) and sulfur (S) lowers Rct. The equivalent circuit shown in the Figure 4.7 includes R1, which contains the solution resistance (R_s), the electrolyte resistance, and other ohmic contributions. C1 represents constant phase element to model non-ideal capacitive behavior. R2 denotes charge transfer resistance (R_ct) which indicates the kinetics of the HER on the surface of the electrode. Lower R_ct is indicative of faster electron transfer and better catalytic activity. C2 is a second series capacitor, which represent additional capacitance, perhaps due to adsorption processes.

The circuit (R1 + (C1 || R2) + C2) is representative of a system with a single dominant charge transfer process (R2) with double-layer effects (C1) and an additional capacitive contribution (C2). This is a common model for HER electrocatalysts,

where the semicircle in the Nyquist plot is characteristic of the charge transfer resistance, and secondary features may represent adsorption or diffusion processes. (Ni, Mo, V)-P, S is the best performing material for HER. It is characterized by the lowest charge transfer resistance (1.2 Ω), which indicates the fastest electron transfer kinetics and highest electrocatalytic activity of the variants examined. The plots exhibit a tail or a second feature, which can be caused by diffusion limitations. (Ni, Mo, V)-P, S has the least pronounced tail, suggesting insignificant diffusion limitations or faster adsorption/desorption kinetics compared to the other variants.

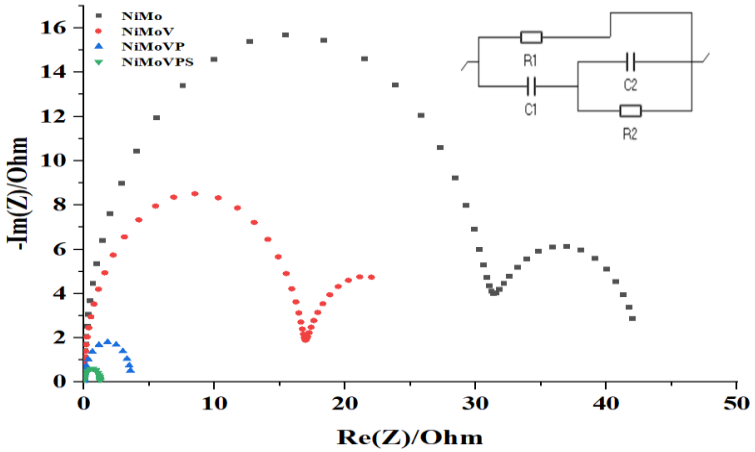

Figure 4. 8: Electrochemical Impedance Spectroscopy (EIS)

4.5.3.3 Tafel analysis

To comprehend the mechanism and kinetics of an electrochemical reaction such as HER, a Tafel plot is utilized. The overpotential and current density are related by the Tafel equation. The Tafel slope was determined from the linear portion of the polarization curve derived via linear sweep voltammetry (LSV). Current density (j) was also transformed to its logarithmic version (log j), and the related overpotential (η) was plotted versus log j to give a Tafel plot. The overpotential was calculated by subtracting the measured electrode potential from the thermodynamic equilibrium potential (0 V for HER). A linear portion of the η vs log j plot was present at moderate overpotential conditions at which kinetic control dominates. In this region, a linear fit was applied and the slope of the fitted line is equal to the Tafel slope (in mV/dec), which is characteristic of the reaction mechanism and the rate-determining step. The tafel slope value reveals the rate-determining step (RDS) of the HER mechanism. All of the electrocatalyst gave a tafel slope of greater than 120mV/dec which indicates that the rate determining step for hydrogen evolution reaction is determined by volmer

step. Out of all the materials tested, the (Ni, Mo, V)-P, S catalyst has the lowest Tafel slope (153.07mV/dec). This is in line with the LSV curves' earlier indication that it is the most active catalyst (requiring least overpotential for a given current density).

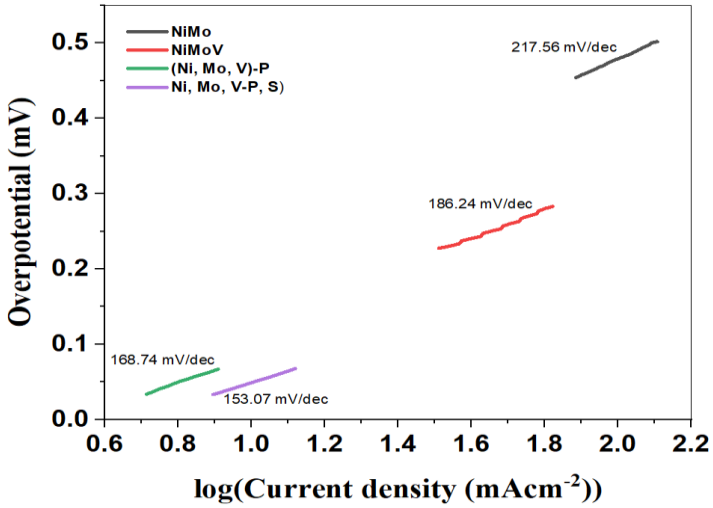

Figure 4. 9: Tafel plot

4.5.3.4 Constant Voltage

The (Ni, Mo, V)-P, S electrocatalyst shows about 30,000 seconds of long-term electrochemical stability, demonstrating continuous operation at a higher current density of 100 mA cm^{-2} at a potential of –242 mV without losing much in its performance. Including under harsh conditions, sustained activity illustrates the strong structural and chemical integrity of the catalyst, which, in other terms, indicates that catalyst surface remains active and unaffected to a large extent by prolonged exposure to the electrolyte or the applied potential. Such stability, in particular, is a requisite condition in large scale hydrogen production where it must continually operate under the current density regime. In other words, this result further confirms the dual advantage of (Ni, Mo, V)-P, S electrocatalyst: intrinsic activity for hydrogen evolution reaction (HER) remains way up while the catalyst remains highly stable in alkaline media. So, it is seen as a very considerable option and therefore can be used in the alkaline water electrolyzer, adding efficiency and operation reliability during work in the long term.

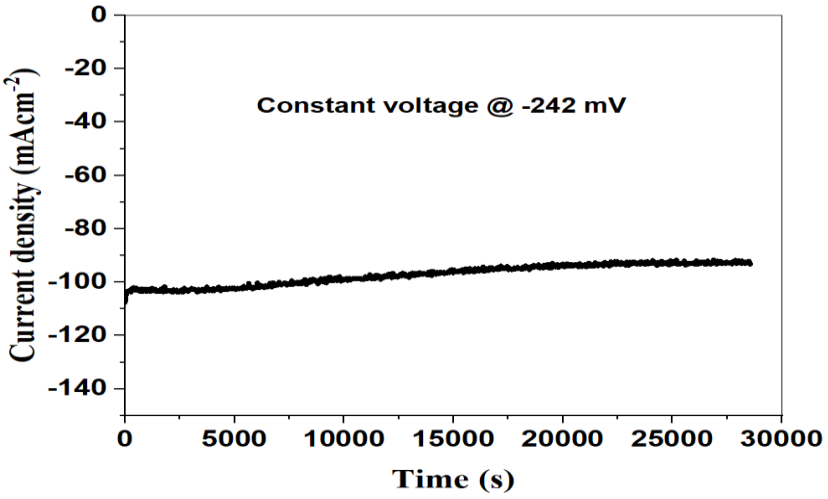

Figure 4. 10: Constant voltage characterizations of (Ni, Mo, V)-P, S

The electrocatalytic performance of the synthesized (Ni, Mo, V)-P, S material was evaluated against both noble metal-based and non-noble metal-based electrocatalysts reported in the literature. At a current density of 10 $mAcm^{-2}$ in 1.0 M KOH, the overpotential (η) of our material is -53 mV with a Tafel slope of 153.07 mV/dec**.** The low overpotential achieved at relatively high current density suggests excellent intrinsic activity for alkaline water electrolysis. Noble metal catalysts Pt/C, Rh_xP/NPC, and Pd-CoSnZn exhibit very low overpotentials (19–36 mV) and significantly lower Tafel slopes (36–70 mV/dec), which point towards high reaction kinetics. In spite of that, the materials are confounded by severe disadvantages based on high cost and availability. On the other hand, non-noble high entropy alloys (HEAs) and transition metal-based catalysts (e.g., NiFeCoCuTi, NiCoFeMnCrP, FeCoNiAlTi) have a broader overpotential window (75–220 mV) and flexible Tafel slopes. Among these, our (Ni, Mo, V)-P, S electrocatalyst stands out by achieving one of the lowest overpotentials (-53 mV) among non-noble metal-based systems in 1.0 M KOH, demonstrating promising performance. In summary, while noble metals maintain kinetic superiority, the synthesized (Ni, Mo, V)-P, S catalyst offers a competitive and practical alternative due to its excellent activity and earth-abundant composition. The performance reinforces its potential as a viable and sustainable candidate for large-scale hydrogen production systems.

Table 4. 4: Comparison of the electrocatalytic activity of the synthesized (Ni, Mo, V)-P, S heterostructure toward HER with previously reported high entropy electrocatalysts.

Electrocatalyst	Electrolyte	η (mV) @10mAcm^{-2}	Reference
(Ni, Mo, V)-P, S	1.0 M KOH	-53	This work
Rh_xP/NPC	0.1 M KOH	-19	(Qin et al., 2018)
Pd-CoSnZn	1.0 M KOH	-30	(Döner et al., 2013)
Pt/C	1.0 M KOH	-36	(Ha et al., 2023)
NiFeCoCuTi	1.0 M KOH	-75	(Shi et al., 2023)
FeCoNiAlTi	1.0 M KOH	-88.2	(Ma et al., 2020)
NiCoFeMnCrP	1.0 M KOH	-220	(Lai et al., 2021)
CoCrFeNiAl	0.5 M H_2SO_4	-73	(Ma et al., 2020)
$Ni_{20}Fe_{20}Mo_{10}Co_{35}Cr_{15}$	0.5 M H_2SO_4	-107	(Zhang et al., 2018)

CHAPTER FIVE
CONCLUSION AND RECOMMENDATION

5.1 Conclusion

In response to the scarcity of affordable alternatives to platinum-group metals, the research highlights the promising performance of multi-element HER electrocatalysts. The study demonstrates the hydrothermal synthesis of nickel foam-supported sulfur and phosphorus co-doped multi-element transition metal electrocatalyst for enhanced hydrogen evolution reaction (HER). The synthesis of the targeted materials was successfully achieved, with characterization confirming the formation of multi-element-doped structures and the uniform incorporation of Ni, Mo, V, S, and P. SEM analysis revealed a porous and roughened surface morphology, beneficial for exposing active sites. XRD was employed to investigate the crystalline structure and phase composition of the synthesized (Ni, Mo, V)-P, S electrocatalyst. EDS and XPS confirmed the presence and distribution of the dopants, while also indicating chemical states induced by co-doping. The study examined the role of non-metal doping concentration on electrocatalyst performance. Optimal doping levels of phosphorus and sulfur were found to substantially enhance HER activity. Electrochemical measurements demonstrated that co-doping with sulfur and phosphorus substantially enhanced HER activity. Among the tested samples, the (Ni, Mo, V)-P, S catalyst exhibited the most promising performance, achieving an overpotential of -53 mV at 10 mA cm^{-2}, and maintaining operational stability about 30,000 seconds at 100 mA cm^{-2}. EIS analysis showed the lowest charge transfer resistance (1.2 Ω), affirming improved electron transport properties. These results indicate that the use of multi-element electrocatalysts is a highly efficient method in promoting HER activity, primarily via the induction of synergy among the elements involved. The synergy lead to better morphology, formation of desirable chemical states and faster charge transfer rates. These improvements are ascribed to synergistic interaction of the dopants, which collectively enhance conductivity, lower reaction energy barriers, and facilitate efficient hydrogen evolution. In conclusion, the study validates that multi-element co-doping of nickel-based catalysts offers an alternative pathway to replace noble metals in alkaline HER applications.

5.2 Recommendation for future work

To establish (Ni, Mo, V)-P, S electrocatalyst as a serious candidate for large-scale hydrogen evolution reaction (HER), a series of follow-up studies are proposed.

1. **Systematic Evaluation across Diverse Electrolyte Environments**

The HER performance and stability of (Ni, Mo, V)-P, S are likely most influenced by the pH of the electrolyte since proton availability, hydrogen adsorption energies, and corrosion susceptibility are likely to be different. Testing the catalyst in acidic, neutral, and alkaline electrolytes will demonstrate its operating flexibility and chemical stability, which are critical to its applicability to various electrolyzer technologies.

2. **Optimization of synthesis parameters**

In order to achieve a significant improvements in the structural and electrochemical behavior of the synthesized electrocatalysts, it is recommended that such parameters as acid cleaning conditions, reaction temperature, time, and pH of precursor solution be independently optimized.

3. **Advanced characterizations and computational modeling**

Advanced characterizations and Density Functional Theory (DFT) modeling are important to fully explain the mechanistic effects of electrocatalyst on HER activity. They can provide atomistic insights into electronic structure, adsorption energies, and reaction mechanisms, complementing experimental results and guiding catalyst design.

4. **Scalability and Benchmarking Studies**

For commercial viability, (Ni, Mo, V)-P, S will have to demonstrate scale-up performance and comparison with state-of-the-art catalysts. Benchmarking and scalability testing will ascertain its commercial viability and guide commercialization.

These studies will elucidate degradation mechanisms, confirm operational flexibility, quantify compositional synergies, and establish industrial feasibility. Through solving these challenges, (Ni, Mo, V)-P, S can be taken to nearer practical implementation in sustainable hydrogen production, helping the global shift to clean energy.

REFERENCES

Alex Martinos, T. S., Laura Cozzi,Víctor García Tapia,Arthur Roge and Davide D'Ambrosio. (2025). *Growth in global energy demand surged in 2024 to almost twice its recent average*. I. Publications.

Altammar, K. A. (2023). A review on nanoparticles: characteristics, synthesis, applications, and challenges. *Frontiers in microbiology*, *14*, 1155622.

Angeles-Olvera, Z., Crespo-Yapur, A., Rodríguez, O., Cholula-Díaz, J. L., Martínez, L. M., & Videa, M. (2022). Nickel-based electrocatalysts for water electrolysis. *Energies*, *15*(5), 1609.

Angelico, R., Giametta, F., Bianchi, B., & Catalano, P. (2025). Green Hydrogen for Energy Transition: A Critical Perspective. *Energies (19961073)*, *18*(2).

Anjum, M. A. R., & Lee, J. S. (2017). Sulfur and nitrogen dual-doped molybdenum phosphide nanocrystallites as an active and stable hydrogen evolution reaction electrocatalyst in acidic and alkaline media. *Acs Catalysis*, *7*(4), 3030-3038.

Araújo, H. F., Gómez, J. A., & Santos, D. M. (2024). Proton-Exchange Membrane Electrolysis for Green Hydrogen Production: Fundamentals, Cost Breakdown, and Strategies to Minimize Platinum-Group Metal Content in Hydrogen Evolution Reaction Electrocatalysts. *Catalysts*, *14*(12), 845.

Asim, M., Hussain, A., Khan, S., Arshad, J., Butt, T. M., Hana, A., Munawar, M., Saira, F., Rani, M., & Mahmood, A. (2022). Sol-gel synthesized high entropy metal oxides as high-performance catalysts for electrochemical water oxidation. *Molecules*, *27*(18), 5951.

Baltrusaitis, J., Mendoza-Sanchez, B., Fernandez, V., Veenstra, R., Dukstiene, N., Roberts, A., & Fairley, N. (2015). Generalized molybdenum oxide surface chemical state XPS determination via informed amorphous sample model. *Applied Surface Science*, *326*, 151-161.

Bang, H. T., Yeo, K. R., Choi, K. J., Jung, W. S., & Kim, S. K. (2022). Ternary Ni-Mo-P catalysts for enhanced activity and durability in proton exchange membrane water electrolysis. *International Journal of Energy Research*, *46*(9), 13023-13034.

Banoth, P., Kandula, C., & Kollu, P. (2022). Introduction to electrocatalysts. In *Noble Metal-Free Electrocatalysts: New Trends in Electrocatalysts for Energy Applications. Volume 2* (pp. 1-37). ACS Publications.

Bau, J. A., Kozlov, S. M., Azofra, L. M., Ould-Chikh, S., Emwas, A.-H., Idriss, H., Cavallo, L., & Takanabe, K. (2020). Role of oxidized Mo species on the active surface of Ni–Mo electrocatalysts for hydrogen evolution under alkaline conditions. *Acs Catalysis*, *10*(21), 12858-12866.

Bhutada, G. (2022). The 200-year history of mankind's energy transitions. World Economic Forum,

Bibi, H., Mansoor, M. A., Asghar, M. A., Ahmad, Z., Numan, A., & Haider, A. (2025). Facile hydrothermal synthesis of highly durable binary and ternary cobalt nickel copper oxides for high-performance oxygen evolution reaction. *International Journal of Hydrogen Energy*, *107*, 369-377.

Bouzbib, M., Rohonczy, J., & Sinkó, K. (2023). Effect of vanadium precursor on dip-coated vanadium oxide thin films. *Journal of Sol-Gel Science and Technology*, *105*(1), 278-290.

Chanturiya, V. A., Bunin, I. Z., & Ryazantseva, M. (2019). XPS study of sulfide minerals surface oxidation under high-voltage nanosecond pulses. *Minerals Engineering*, *143*, 105939.

Chaudhari, N. K., Jin, H., Kim, B., & Lee, K. (2017). Nanostructured materials on 3D nickel foam as electrocatalysts for water splitting. *Nanoscale*, *9*(34), 12231-12247.

Chigbu, U. E., & Nweke-Eze, C. (2023). Green hydrogen production and its land tenure consequences in Africa: An Interpretive review. *Land*, *12*(9), 1709.

De, A., Kim, M. S., Adhikari, A., Patel, R., & Kundu, S. (2024). Sol-gel derived nanostructure electrocatalysts for oxygen evolution reaction: A review. *Journal of Materials Chemistry A*.

Döner, A., Tezcan, F., & Kardaş, G. (2013). Electrocatalytic behavior of the Pd-modified electrocatalyst for hydrogen evolution. *International Journal of Hydrogen Energy*, *38*(10), 3881-3888.

Ďurovič, M., Hnát, J., & Bouzek, K. (2021). Electrocatalysts for the hydrogen evolution reaction in alkaline and neutral media. A comparative review. *Journal of Power Sources*, *493*, 229708.

Elgrishi, N., Rountree, K. J., McCarthy, B. D., Rountree, E. S., Eisenhart, T. T., & Dempsey, J. L. (2018). A practical beginner's guide to cyclic voltammetry. *Journal of chemical education*, *95*(2), 197-206.

Esposito, S. (2019). "Traditional" sol-gel chemistry as a powerful tool for the preparation of supported metal and metal oxide catalysts. *Materials*, *12*(4), 668.

Fan, H., Li, F., & Xu, A. (2025). Green Hydrogen Economy: Scenarios versus Technologies. *Energy & Fuels*.

Fang, M., Gao, W., Dong, G., Xia, Z., Yip, S., Qin, Y., Qu, Y., & Ho, J. C. (2016). Hierarchical NiMo-based 3D electrocatalysts for highly-efficient hydrogen evolution in alkaline conditions. *Nano Energy*, *27*, 247-254.

Farsadrooh, M., Yazdan-Abad, M. Z., Noroozifar, M., Alfi, N., & Modarresi-Alam, A. R. (2020). Fast improved polyol method for synthesis of Pd/C catalyst with high performance toward ethanol electrooxidation. *International Journal of Hydrogen Energy*, *45*(51), 27312-27319.

Fathyunes, L., Muilwijk, C., & Brabazon, D. (2024). Hydrothermal synthesis of (NiFe/NiCo) S@ NF bilayer electrocatalyst for efficient hydrogen evolution reaction. *International Journal of Hydrogen Energy*, *78*, 622-633.

García-Contreras, M. A., & Fernández-Valverde, S. M. (2011). Electrocatalysts of Pt-TiO2 prepared by sol-gel and microwave-assisted polyol method for the oxygen reduction reaction in 0.5 M H2SO4. *Journal of Microwave Power and Electromagnetic Energy*, *45*(4), 188-192.

Genc, T. S., & Kosempel, S. (2023). Energy transition and the economy: a review article. *Energies*, *16*(7), 2965.

Ghosn, F., Zreik, M., Awad, G., & Karouni, G. (2024). Energy transition and sustainable development in Malaysia: Steering towards a greener future. *International Journal of Renewable Energy Development*, *13*(3), 362-374.

Giovanni Andrean, S. B., Herib Blanco, S., Budinis, J. C., Elizabeth , Connelly, C. D., Stavroula , Evangelopoulou, M. F., & Alexandre Gouy, R. M. G., Shane McDonagh, Megumi Kotani, Francesco Pavan, Amalia Pizarro, Richard Simon and Deniz Ugur (2025). *Global Hydrogen Review 2024*.

Guta, D., & Börner, J. (2017). Energy security, uncertainty and energy resource use options in Ethiopia: A sector modelling approach. *International Journal of Energy Sector Management*, *11*(1), 91-117.

Guzman-Bucio, D. M., Gomez-Sosa, G., Cabrera-German, D., Torres-Ochoa, J. A., Bravo-Sanchez, M., Cortazar-Martinez, O., Carmona-Carmona, A. J., & Herrera-Gomez, A. (2023). Detailed peak fitting analysis of the Ni 2p photoemission spectrum for metallic nickel and an initial oxidation. *Journal of Electron Spectroscopy and Related Phenomena*, *262*, 147284.

Ha, Q.-N., Gultom, N. S., Silitonga, M. Z., Gemeda, T. N., & Kuo, D.-H. (2023). Novel core–shell structure of Ni3S2@ LiMoNiOx (OH) y nanorod arrays toward efficient high-current–density hydrogen evolution reaction. *Chemical Engineering Journal*, *467*, 143253.

Hassan, Q., Viktor, P., Al-Musawi, T. J., Ali, B. M., Algburi, S., Alzoubi, H. M., Al-Jiboory, A. K., Sameen, A. Z., Salman, H. M., & Jaszczur, M. (2024). The renewable energy role in the global energy Transformations. *Renewable Energy Focus*, *48*, 100545.

Hodoroaba, V.-D. (2020). Energy-dispersive X-ray spectroscopy (EDS). In *Characterization of nanoparticles* (pp. 397-417). Elsevier.

Hydrogen. (2025). https://doi.org/https://www.irena.org/Energy-Transition/Technology/Hydrogen

Ibekwe, K. I., Etukudoh, E. A., Nwokediegwu, Z. Q. S., Umoh, A. A., Adefemi, A., & Ilojianya, V. I. (2024). Energy security in the global context: A comprehensive review of geopolitical dynamics and policies. *Engineering Science & Technology Journal*, *5*(1), 152-168.

Jayaseelan, C., Rahuman, A. A., Ramkumar, R., Perumal, P., Rajakumar, G., Kirthi, A. V., Santhoshkumar, T., & Marimuthu, S. (2014). Effect of sub-acute exposure to nickel nanoparticles on oxidative stress and histopathological changes in Mozambique tilapia, Oreochromis mossambicus. *Ecotoxicology and Environmental Safety*, *107*, 220-228.

Jeon, J.-H., Kim, J.-E., Kim, T.-H., Park, C.-S., Jung, K., Yoon, J., Kim, J., Kim, Y.-H., & Kang, K.-S. (2024). Enhanced oxygen evolution reaction in hierarchical NiFe/NiO electrocatalysts: Effects of electrodeposition condition on electrode. *Electrochemistry Communications*, *160*, 107668.

Jia, F., Zou, X., Wei, X., Bao, W., Ai, T., Li, W., & Guo, Y. (2023). Synergistic effect of P doping and Mo-Ni-based heterostructure electrocatalyst for overall water splitting. *Materials*, *16*(9), 3411.

Kamel, M. M., Abd-Ellah, A. A., Alhadhrami, A., Ibrahim, M. M., Anwer, Z. M., Shata, S. S., & Mostafa, N. Y. (2025). Ni–Mo nanostructure alloys as effective electrocatalysts for green hydrogen production in an acidic medium. *RSC advances*, *15*(2), 1344-1357.

Khan, B., & Singh, P. (2017). The current and future states of Ethiopia's energy sector and potential for green energy: A comprehensive study. *International Journal of Engineering Research in Africa*, *33*, 115-139.

Khan, N., Kalair, E., Abas, N., Kalair, A., & Kalair, A. (2019). Energy transition from molecules to atoms and photons. *Engineering Science and Technology, an International Journal*, *22*(1), 185-214.

Kim, H., Hong, S., Bang, J., Jun, Y., Choe, S., Kim, S. Y., & Ahn, S. H. (2024). Self-terminated electrodeposition of Pt group metal: principles, synthetic strategies, and applications. *Energy Materials*, *4*(1).

Kim, J., Jang, Y. J., & Jang, Y. H. (2023). Electrodeposition of Stable Noble-Metal-Free Co-P Electrocatalysts for Hydrogen Evolution Reaction. *Materials*, *16*(2), 593.

Kim, Y., Jun, S. E., Lee, G., Nam, S., Jang, H. W., Park, S. H., & Kwon, K. C. (2023). Recent advances in water-splitting electrocatalysts based on electrodeposition. *Materials*, *16*(8), 3044.

Kuriganova, A., Faddeev, N., Gorshenkov, M., Kuznetsov, D., Leontyev, I., & Smirnova, N. (2020). A comparison of "bottom-up" and "top-down" approaches to the synthesis of Pt/C electrocatalysts. *Processes*, *8*(8), 947.

Lai, D., Kang, Q., Gao, F., & Lu, Q. (2021). High-entropy effect of a metal phosphide on enhanced overall water splitting performance. *Journal of Materials Chemistry A*, *9*(33), 17913-17922.

Lazanas, A. C., & Prodromidis, M. I. (2023). Electrochemical impedance spectroscopy– a tutorial. *ACS measurement science au*, *3*(3), 162-193.

Li, C., & Baek, J.-B. (2019). Recent advances in noble metal (Pt, Ru, and Ir)-based electrocatalysts for efficient hydrogen evolution reaction. *ACS omega*, *5*(1), 31-40.

Lima, V. S., Almeida, T. S., & De Andrade, A. R. (2023). Glycerol electro-oxidation in alkaline medium with Pt-Fe/C electrocatalysts synthesized by the polyol method: Increased selectivity and activity provided by less expensive catalysts. *Nanomaterials*, *13*(7), 1173.

Liu, Y., Wang, H., Yuan, X., Wu, Y., Wang, H., Tan, Y. Z., & Chew, J. W. (2021). Roles of sulfur-edge sites, metal-edge sites, terrace sites, and defects in metal sulfides for photocatalysis. *Chem Catalysis*, *1*(1), 44-68.

Lou, F., & Chen, D. (2015). Aligned carbon nanostructures based 3D electrodes for energy storage. *Journal of Energy Chemistry*, *24*(5), 559-586.

Ma, P., Zhao, M., Zhang, L., Wang, H., Gu, J., Sun, Y., Ji, W., & Fu, Z. (2020). Self-supported high-entropy alloy electrocatalyst for highly efficient H2 evolution in acid condition. *Journal of Materiomics*, *6*(4), 736-742.

Magar, H. S., Hassan, R. Y., & Mulchandani, A. (2021). Electrochemical impedance spectroscopy (EIS): Principles, construction, and biosensing applications. *Sensors*, *21*(19), 6578.

Mahabari, K., Mohili, R. D., Patel, M., Jadhav, A. H., Lee, K., & Chaudhari, N. K. (2024). HF-free microwave-assisted synthesis of MXene as an electrocatalyst for hydrogen evolution in alkaline media. *Nanoscale Advances*, *6*(21), 5388-5397.

Mahmood, N., Yao, Y., Zhang, J. W., Pan, L., Zhang, X., & Zou, J. J. (2018). Electrocatalysts for hydrogen evolution in alkaline electrolytes: mechanisms, challenges, and prospective solutions. *Advanced science*, *5*(2), 1700464.

Martínez-Lázaro, A., Mendoza-Camargo, A., Rodriguez-Barajas, M., Espinosa-Lagunes, F., Salazar-Lara, Y., Herrera-Gomez, A., Cortazar-Martínez, O., Rey-Raap, N., Ledesma-García, J., & Arenillas, A. (2023). Effective Synthesis Procedure Based on Microwave Heating of the PdCo Aerogel Electrocatalyst for Its Use in Microfluidic Devices. *ACS Applied Energy Materials*, *6*(12), 6410-6418.

Miao, M., Duan, H., Luo, J., & Wang, X. (2022). Recent progress and prospect of electrodeposition-type catalysts in carbon dioxide reduction utilizations. *Materials Advances*, *3*(18), 6968-6987.

Mikulčić, H., Baleta, J., Klemeš, J. J., & Wang, X. (2021). Energy transition and the role of system integration of the energy, water and environmental systems. *Journal of Cleaner Production*, *292*, 126027.

Moradi, K., Ashrafi, M., Salimi, A., & Melander, M. (2024). Hierarchical MoS2@ NiFeCo-Mo (doped)-LDH Heterostructures as Efficient Alkaline Water Splitting (Photo) Electrocatalysts.

Nacys, A., Kilmonis, T., Kepenienė, V., Balčiūnaitė, A., Stagniūnaitė, R., Upskuvienė, D., Jablonskienė, J., Vaičiūnienė, J., Skapas, M., & Tamašauskaitė-Tamašiūnaitė, L. (2021). One-Pot Microwave-Assisted Synthesis of Graphene-Supported PtCoM (M= Mn, Ru, Mo) Catalysts for Low-Temperature Fuel Cells. *Catalysts*, *11*(12), 1431.

Napporn, T. W., Holade, Y., Kokoh, B., Mitsushima, S., Mayer, K., Eichberger, B., & Hacker, V. (2018). Electrochemical measurement methods and characterization on the cell level. In *Fuel Cells and Hydrogen* (pp. 175-214). Elsevier.

Ndlwana, L., Raleie, N., Dimpe, K. M., Ogutu, H. F., Oseghe, E. O., Motsa, M. M., Msagati, T. A., & Mamba, B. B. (2021). Sustainable hydrothermal and solvothermal synthesis of advanced carbon materials in multidimensional applications: A review. *Materials*, *14*(17), 5094.

Ni, B., & Wang, X. (2015). Face the edges: catalytic active sites of nanomaterials. *Advanced science*, *2*(7), 1500085.

NIST X-ray Photoelectron Spectroscopy Database (SRD 20), Version 5.0 ((2023). https://srdata.nist.gov/xps/

Patil, R. B., Mantri, A., House, S. D., Yang, J. C., & McKone, J. R. (2019). Enhancing the performance of Ni-Mo alkaline hydrogen evolution electrocatalysts with carbon supports. *ACS Applied Energy Materials*, *2*(4), 2524-2533.

Pavlets, A., Alekseenko, A., Menshchikov, V., Belenov, S., Volochaev, V., Pankov, I., Safronenko, O., & Guterman, V. (2021). Influence of electrochemical pretreatment conditions of PtCu/C alloy electrocatalyst on its activity. *Nanomaterials*, *11*(6), 1499.

Pearson, P. J. (2018). Past, present and prospective energy transitions: an invitation to historians. *Revue d'Histoire de l'Énergie*, *1*(1), 1d-28d.

Pepe, J. M., Ansari, D., & Gehrung, R. M. (2023). The geopolitics of hydrogen: Technologies, actors and scenarios until 2040.

Petkucheva, E. S., Mladenova, B., Muhyuddin, M., Dimitrova, M., Borisov, G. R., Santoro, C., & Slavcheva, E. (2025). Sol–Gel-Synthesized Pt, Ni and Co-Based Electrocatalyst Effects of the Support Type, Characterization, and Possible Application in AEM-URFC. *Gels*, *11*(4), 229.

Qin, Q., Jang, H., Chen, L., Nam, G., Liu, X., & Cho, J. (2018). Low loading of RhxP and RuP on N, P codoped carbon as two trifunctional electrocatalysts for the oxygen and hydrogen electrode reactions. *Advanced Energy Materials*, *8*(29), 1801478.

Rafiaei, S. M. (2018). The luminescence properties of yttria based phosphors and study of YBO3 formation via H3BO3 addition. *Processing and Application of Ceramics*, *12*(3), 262-267.

Rafiee, M., Abrams, D. J., Cardinale, L., Goss, Z., Romero-Arenas, A., & Stahl, S. S. (2024). Cyclic voltammetry and chronoamperometry: mechanistic tools for organic electrosynthesis. *Chemical Society Reviews*, *53*(2), 566-585.

Rashid, U., Ma, X., Zhu, Y., Cao, C., & Zou, M. (2025). The Comprehensive Review of Cobalt Based Electrocatalysts Synthesized via new Microwave Assisted Methodology. *Materials Chemistry Frontiers*.

Raveendran, A., Chandran, M., & Dhanusuraman, R. (2023). A comprehensive review on the electrochemical parameters and recent material development of electrochemical water splitting electrocatalysts. *RSC advances*, *13*(6), 3843-3876.

Rossi, R., Nicolas, J., & Logan, B. E. (2023). Using nickel-molybdenum cathode catalysts for efficient hydrogen gas production in microbial electrolysis cells. *Journal of Power Sources*, *560*, 232594.

Roychowdhury, C., Matsumoto, F., Mutolo, P. F., Abruña, H. D., & DiSalvo, F. J. (2005). Synthesis, characterization, and electrocatalytic activity of PtBi nanoparticles prepared by the polyol process. *Chemistry of Materials*, *17*(23), 5871-5876.

Salunkhe, P., AV, M. A., & Kekuda, D. (2020). Investigation on tailoring physical properties of Nickel Oxide thin films grown by dc magnetron sputtering. *Materials Research Express*, *7*(1), 016427.

Schneider, L. P. C., Dhrioua, M., Ullmer, D., Egert, F., Wiggenhauser, H. J., Ghotia, K., Kawerau, N., Grilli, D., Razmjooei, F., & Ansar, S. A. (2024). Advancements in Hydrogen Production using Alkaline Electrolysis Systems: A Short Review on Experimental and Simulation Studies. *Current Opinion in Electrochemistry*, 101552.

Sebbahi, S., Assila, A., Belghiti, A. A., Laasri, S., Kaya, S., Hlil, E. K., Rachidi, S., & Hajjaji, A. (2024). A comprehensive review of recent advances in alkaline water electrolysis for hydrogen production. *International Journal of Hydrogen Energy*, *82*, 583-599.

Shen, W., Ye, Y., Xia, Q., & Xi, P. (2025). Progress in in situ characterization of electrocatalysis. *EES Catalysis*, *3*(1), 10-31.

Shi, H., Sun, X.-Y., Zeng, S.-P., Liu, Y., Han, G.-F., Wang, T.-H., Wen, Z., Fang, Q.-R., Lang, X.-Y., & Jiang, Q. (2023). Nanoporous nonprecious high-entropy alloys as multisite electrocatalysts for ampere-level current-density hydrogen evolution. *Small Structures*, *4*(9), 2300042.

Shi, J., Bao, Y., Ye, R., Zhong, J., Zhou, L.-J., Zhao, Z., Kang, W., & Aidarova, S. B. (2025). Recent progress and perspective of electrocatalysts for hydrogen evolution reaction. *Catalysis Science & Technology*.

Silversmit, G., Depla, D., Poelman, H., Marin, G. B., & De Gryse, R. (2004). Determination of the V2p XPS binding energies for different vanadium oxidation states (V5+ to V0+). *Journal of Electron Spectroscopy and Related Phenomena*, *135*(2-3), 167-175.

Singh, A. (2025). *Top 10 Hydrogen Developments in 2024*.

Singu, B. S., Mandal, D., Sim, J. E., & Kim, H. (2024). Synthesis of Stable and Efficient Electrocatalysts for Hydrogen Evolution: Hierarchical NiMo-Based Hollow Nanotubes. *International Journal of Energy Research*, *2024*(1), 7724598.

Solangi, M. Y., Lakhair, A. A., Dayo, F. Z., Qureshi, R. A., Alhazaa, A., Shar, M. A., Laghari, A. J., Soomro, I. A., Lakhan, M. N., & Hanan, A. (2024). Ti 3 C 2 T x MXene coupled Co (OH) 2: a stable electrocatalyst for the hydrogen evolution reaction in alkaline media. *RSC Sustainability*, *2*(11), 3424-3435.

Suleiman, M., Al-Masri, M., Al Ali, A., Aref, D., Hussein, A., Saadeddin, I., & Warad, I. (2015). Synthesis of nano-sized sulfur nanoparticles and their antibacterial activities. *J Mater Environ Sci*, *6*(2), 513-518.

Tiruye, G., Besha, A., Mekonnen, Y., Benti, N., Gebreslase, G., & Tufa, R. (2021). Opportunities and Challenges of Renewable Energy Production in Ethiopia. Sustainability 2021, 13, 10381. In: s Note: MDPI stays neutral with regard to jurisdictional claims in published ….

Tiruye, G. A., Besha, A. T., Mekonnen, Y. S., Benti, N. E., Gebreslase, G. A., & Tufa, R. A. (2021). Opportunities and challenges of renewable energy production in Ethiopia. *Sustainability*, *13*(18), 10381.

van der Heijden, O., Park, S., Vos, R. E., Eggebeen, J. J., & Koper, M. T. (2024). Tafel slope plot as a tool to analyze electrocatalytic reactions. *ACS Energy Letters*, *9*(4), 1871-1879.

Velázquez-Hernández, I., Álvarez-Contreras, L., Guerra-Balcázar, M., & Arjona, N. (2023). Oxygen defects in metal oxides and their impact on the electrochemical oxidation of short-chain alcohols. In *Metal Oxide Defects* (pp. 453-490). Elsevier.

Vij, V., Sultan, S., Harzandi, A. M., Meena, A., Tiwari, J. N., Lee, W.-G., Yoon, T., & Kim, K. S. (2017). Nickel-based electrocatalysts for energy-related applications: oxygen reduction, oxygen evolution, and hydrogen evolution reactions. *Acs Catalysis*, *7*(10), 7196-7225.

Vinodh, R., Palanivel, T., Kalanur, S. S., & Pollet, B. G. (2024). Recent advancements in catalyst coated membranes for water electrolysis: a critical review. *Energy Advances*, *3*(6), 1144-1166.

Wan, J., Zhang, Q., Liu, E., Chen, Y., Zheng, J., Ren, A., Drisdell, W. S., & Zheng, H. (2025). In-situ/operando study of Cu-based nanocatalysts for CO2 electroreduction using electrochemical liquid cell TEM. *Frontiers in Chemistry*, *13*, 1525245.

Wang, C. R., Stansberry, J. M., Mukundan, R., Chang, H.-M. J., Kulkarni, D., Park, A. M., Plymill, A. B., Firas, N. M., Liu, C. P., & Lang, J. T. (2025). Proton Exchange Membrane (PEM) Water Electrolysis: Cell-Level Considerations for Gigawatt-Scale Deployment. *Chemical Reviews*.

Wang, F., Xiao, L., Jiang, Y., Liu, X., Zhao, X., Kong, Q., Abdukayum, A., & Hu, G. (2025). Recent achievements in noble metal-based oxide electrocatalysts for water splitting. *Materials Horizons*.

Wang, J., Mueller, D. N., & Crumlin, E. J. (2024). Recommended strategies for quantifying oxygen vacancies with X-ray photoelectron spectroscopy. *Journal of the European Ceramic Society*, 116709.

Wang, S., Lu, A., & Zhong, C.-J. (2021). Hydrogen production from water electrolysis: role of catalysts. *Nano Convergence*, *8*(1), 4.

Wu, H., Chen, M., Cheng, H., Yang, T., Zeng, M., & Yang, M. (2025). Interpretable physics-informed machine learning approaches to accelerate electrocatalyst development. *Journal of materials informatics*, *5*(2).

Xie, S., Dong, H., Peng, X., & Chu, P. K. (2024). Non-precious electrocatalysts for the hydrogen evolution reaction. *Innov. Discov.*, *1*, 11.

Xu, W., Li, S.-J., Wang, J.-N., Peng, B., Yin, W.-J., Tang, X., & Shen, Y. (2024). Introducing active sites and regulating electron distribution to design Mo and P co-doped Ni for efficient alkaline hydrogen evolution reaction. *Molecular Catalysis*, *559*, 114069.

Yalew, A. W. (2022). The Ethiopian energy sector and its implications for the SDGs and modeling. *Renewable and Sustainable Energy Transition*, *2*, 100018.

Yang, S., Liu, Z., Wan, P., Liu, L., Sun, Y., Xiao, F., Wang, S., & Xiao, J. (2024). Exploring the degradation mechanism of nickel–copper–molybdenum hydrogen evolution catalysts during intermittent operation. *Chemical Communications*, *60*(1), 59-62.

Yasmina Abdelilah, A. A. B., Vasilios Anatolitis, H. B., Piotr Bojek, François Briens, Trevor Criswell, , & Jeremy Moorhouse, K. V., and Laura Mari Martinez. (2025). *Renewables 2024 Analysis and forecast to 2030*.

You, B., & Qiao, S. Z. (2021). Destabilizing Alkaline Water with 3d-Metal (Oxy)(Hydr) Oxides for Improved Hydrogen Evolution. *Chemistry–A European Journal*, *27*(2), 553-564.

Zhai, W., Ma, Y., Chen, D., Ho, J. C., Dai, Z., & Qu, Y. (2022). Recent progress on the long-term stability of hydrogen evolution reaction electrocatalysts. *InfoMat*, *4*(9), e12357.

Zhang, G., Ming, K., Kang, J., Huang, Q., Zhang, Z., Zheng, X., & Bi, X. (2018). High entropy alloy as a highly active and stable electrocatalyst for hydrogen evolution reaction. *Electrochimica Acta*, *279*, 19-23.

Zhang, H.-M., Zhang, S.-F., Zuo, L.-H., Li, J.-K., Guo, J.-X., Wang, P., Sun, J.-F., & Dai, L. (2024). Recent advances of high-entropy electrocatalysts for water electrolysis by electrodeposition technology: a short review. *Rare Metals*, *43*(6), 2371-2390.

Zhang, X., Guo, Y., & Wang, C. (2024). Multi-interface engineering of nickel-based electrocatalysts for alkaline hydrogen evolution reaction. *Energy Materials*, *4*(4), N/A-N/A.

Zheng, W., Li, Y., Tsang, C.-S., So, P.-K., & Lee, L. Y. S. (2021). Stabilizer-free bismuth nanoparticles for selective polyol electrooxidation. *Iscience*, *24*(4).

Zhu, P., Ye, L., Li, X., Wang, T., Zhong, Y., & Zhuang, L. (2024). Ni3S2 particle–embedded nanotubes as a high-performance electrocatalyst for overall water splitting. *APL Materials*, *12*(9).

Zhu, Y., Li, L., Cheng, H., & Ma, J. (2024). Alkaline Hydrogen Evolution Reaction Electrocatalysts for Anion Exchange Membrane Water Electrolyzers: Progress and Perspective. *JACS Au*, *4*(12), 4639-4654.

Zoulias, E., Varkaraki, E., Lymberopoulos, N., Christodoulou, C. N., & Karagiorgis, G. N. (2004). A review on water electrolysis. *Tcjst*, *4*(2), 41-71.

Research Fund Acknowledgement

This thesis work is funded by Adama Science and Technology University under grant number ASTU/SM-R/1089/25.